THE PENNSYLVANIA
STATE UNIVERSITY

IONOSPHERIC RESEARCH

Scientific Report No. 158

A WIDE APERTURE, HIGH DIRECTIVITY, SCANNED ANTENNA ARRAY

by

Alfred B. Gschwendtner

April 1, 1962

PROJECT WINDS

IONOSPHERE RESEARCH LABORATORY

University Park, Pennsylvania

Contract No. NSF-G14246

IONOSPHERE RESEARCH

Contract No. NSF-G14246

SCIENTIFIC REPORT

on

A Wide Aperture, High Directivity, Scanned Antenna Array

by

Alfred B. Gschwendtner

April 1, 1962

Scientific Report No. 158

IONOSPHERE RESEARCH LABORATORY
PROJECT WINDS

Submitted by: Sidney A. Bowhill

S. A. Bowhill, Associate Professor of Electrical Engineering, Project Supervisor

Approved by: A. H. Waynick

A. H. Waynick, Professor of Electrical Engineering, Director, IRL

THE PENNSYLVANIA STATE UNIVERSITY

College of Engineering and Architecture

Department of Electrical Engineering

TABLE OF CONTENTS

ABSTRACT

This report deals with instrumentation developed to record the complex amplitude distribution of pulsed radio waves after reflection by the ionosphere. The method of recording has as its basis a semiconductor switch which provides rapid scanning of six antennas placed in a linear array. Although observations are currently being made visually with film recording, provisions have been made for changeover to a digital recording method for analysis by a high speed computer.

Complete descriptions of the various parts of the equipment are given, and preliminary results obtained by the visual method are shown.

LIST OF FIGURES

LIST OF SYMBOLS

A_o = magnitude of in phase component

A_1 = magnitude of quadrature component

C = curve of integration

E = electric field

H = magnetic field

J = current

P = angular spectrum

T = tangential

V = rectangular component of a field vector

a = discrete point on x axis

c = velocity of light, $\cos\alpha$

e = base of Naperian logarithms

g = general function

$i = \sqrt{-1}$

$k = \frac{2\pi}{\lambda}$

$k_o = \frac{2\pi}{\lambda_o}$

m = milli

p = optical path, function of r,θ

r = spherical coordinate

s = $\sin\alpha$

t = time

x,y,z = spsce rectangular coordinates

α = angle between wave normal and x axis

β = $\cos\alpha$

γ = general point on x axis

η = index of refraction = $\sqrt{\varepsilon\mu}$

ε = permittivity of space

ρ = correlation coefficient

λ = wavelength

λ_o = free space wavelength

θ = spherical coordinate

ϕ = phase of wave

μ = permeability of space, micro

CHAPTER I

INTRODUCTION

Radio waves observed after reflection from the ionosphere exhibit fluctuations in amplitude and phase. A large body of investigations, which will be treated shortly, indicates that these fluctuations are caused by patches of ionization which are more dense than the ambient level of the surrounding ionosphere. A form of representation of this dense patch of ionization or irregularity is a thin screen which alters the amplitude and phase of a radio wave passing through it. If the wave incident on the screen were a plane wave, before passing through the screen the equiphase points or wavefront would be a straight line. Upon emergence from the screen, the wavefront would be a random curve. Because of diffractive changes, the form of this curve varies with distance from the screen. The wavefront observed on the ground corresponds to the diffraction pattern of physical optics.

Any study of the nature of ionospheric irregularities by ground based radio transmitters and receivers must include, therefore, an analysis of the diffraction pattern. This pattern can be measured by a number of receivers whose separation is sufficiently large to resolve the structure of the wavefront. The wide aperture, high directivity, scanned antenna array, to be described in this study, provides a ready means of studying the diffraction pattern.

A. PREVIOUS RELATED STUDIES

Ratcliffe and Pawsey[1] observed the amplitude fluctuations of ionospherically reflected waves with spaced receivers. They found that the closer the receivers were to each other the more similar were the amplitude variations, and the farther away they were the more dissimilar. They suggested that the amplitude differences between antennas were caused by diffraction and that the fading or fluctuation was caused by a motion of the diffracting irregularity. Pawsey,[2] using a spaced receiver method, made the first measure of the speed of an irregularity. He measured the time difference between related maxima at two receivers a known distance apart and from this computed the drift velocity of the irregularity in the ionosphere. Ratcliffe,[3] basing his theory on the mathematical analysis of random noise by Rice,[4] compared the fading of reflected radio waves to the problem of passing random noise through a filter. Booker, Ratcliffe and Shinn[5] analyzed the diffraction effects produced when a plane wave is incident upon a diffracting screen which is irregular in the horizontal direction. They also related the diffraction pattern to a generalized spatial autocorrelation function which is invariant with distance from the diffracting screen. Booker and Clemmow[6] related the concept of an angular spectrum of plane waves to the polar diagram of an antenna and to the distribution of waves emerging after diffraction at an aperture.

Briggs, Phillips and Shinn[7] developed a method for taking into account the effects of drift and random velocity by autocorrelation analysis.

Bramley[8] developed the theory of a random cone of downcoming waves employing methods introduced by Rice[4] for the analogous problem of time varying noise. He also derived expressions particularly suited to analysis of direction finding errors. Hewish,[9] basing his analysis on radio star scintillations, discussed the problem of a radio wave passing through a thin phase changing screen. In a later paper Hewish[10] developed the theory for determining the height of irregularities from observations of the amplitude and phase of extraterrestrial radio waves. Fejer[11] deduced the angular spectrum produced when a wave passes through a thick medium containing weak irregularities of electron density with a two-dimensional Gaussian autocorrelation function. For the case of weak scatter by the medium, the amplitude of the signal a long way from the screen was shown to have a displaced Gaussian probability distribution. For the case of strong scatter the amplitude of the signal at a great distance had a Rayleigh distribution. Bramley[12] arrived at a result identical to Fejer[11] by assuming the medium to be a single, thin, deeply modulated phase screen of the type treated by Hewish.[9,10] Jones, Millman and Mertney[13] attempted to locate the region in the ionosphere in which the irregularities causing the fading of 150 kc/s

radio waves are situated. Assuming that the irregularities are below the level of reflection and assuming that the field below the irregularity is the same as the field at the ground, the ratio of amplitude to phase change measured at the ground determines the height of the irregularity through the known variation of collision frequency with height. Bowhill[14] considered the fading of radio waves between 16 and 2400 kc/s. Experiments based on vertical incidence measurements at 70 and 85 kc/s indicated that the diffraction effects were different for different frequencies. Ratcliffe[15] summarised existing papers relevant to the field of diffraction in the ionosphere.

Houston[16] measured phase changes of a pulsed radio signal at 75 kc/s incident vertically on the ionosphere. He developed a method of phase comparison for pulsed signals which is basic to the phase measuring components of the wide aperture antenna system described in this study. Pitteway[17] investigated the scattering of a wave which accompanies reflection from a stratified ionosphere containing weak irregularities. He assumed that the irregularities are confined to a thin layer near a given height and examined the possibility that increased scattering might be brought about if the height of the layer were near the height of reflection of the wave. This was not found to be the case.

Bowhill[18] considered the scattering of an electromagnetic wave by a continuous medium containing three-

dimensional random inhomogeneities of refractive index. The form of the angular power spectrum was derived for the case of anisotropic scales of the inhomogeneities in the three space directions. In a later paper Bowhill[19] developed the mathematical tools for studying the statistical properties of a random signal diffracting in free space. Hargreaves,[20] using spaced receivers and monitoring amplitude and phase fluctuations at 16 kc/s after reflection from the ionosphere, deduced that the ionosphere modulates the phase rather than the amplitude of the wave. Moreover, he found that a model of the ionosphere in which the reflection coefficient is constant and the height of reflection fluctuates conformed with observed fluctuations at the ground.

B. STATEMENT OF THE PROBLEM AND DEFINITION OF TERMS

The specific problem to be solved in this study is the development of a technique for studying the angular spectrum of ionospherically reflected waves. The angular spectrum, which will be more fully discussed in Chapter IV, is produced when an electromagnetic wave passes through a thin diffracting screen. It is defined as an aggregate of infinite plane waves traveling in all directions. Each of the component waves travels in its own direction independently. At any plane parallel to the diffracting plane the components of the angular spectrum arrive with phase differences depending on their direction. The wave assembly

adds to form a distribution of complex amplitude which is different for each plane.

Diffraction may be defined, therefore, as the interference effect produced by spreading electromagnetic waves in free space, and the diffracting screen may be defined as any disturbance which gives rise to these effects when interposed between the source of the wave and the observer.

In physical optics two types of diffraction are commonly discussed: Fresnel and Fraunhofer diffraction. The transition from one type to the other is a function of the distance of the observer from the diffracting screen. Specifically,[21] distances less than $\frac{2D^2}{\lambda}$, where D is the horizontal extent of the diffracting screen and λ is the wavelength of the incident radiation, are within the Fresnel region. Distances from the screen greater than $\frac{2D^2}{\lambda}$ are within the Fraunhofer region. The wavelength of the diffraction pattern being investigated by the technique described in this study is 1 km. A measurement of the pulse delay encountered in reflection from the ionosphere indicates that the height of reflection is about 100 km. Assuming that the irregularities acting as diffracting screens are below the height of reflection and that their horizontal dimensions are on the order of 5 km, the expression above indicates that the diffraction problem is a Fraunhofer diffraction problem.

Because it serves as a first principle approach to the concept of an angular spread of waves emerging from an irregularity after a plane wave is incident upon it, geometrical optics will also be discussed in Chapter IV. Geometrical optics is that branch of physics which treats an electromagnetic disturbance as if it were composed of rays diverging in various directions from the source and abruptly returned after reflection or refraction from a surface. In short, geometrical optics neglects the wavelength of the wave being studied. Obviously, the existence of diffracting or spreading effects as well as scattering tends to invalidate the ray approach when the incident wavelength is on the order of the dimensions of the disturbing body. Scattering, on the other hand, is a randomization brought about by reflection from a rough surface.

Diffracting screens may produce amplitude, phase, or amplitude and phase variations on an incident plane wave. In this study consideration will be given only to shallow amplitude and phase screens. According to one definition,[14] a phase screen is deep or shallow depending on whether the phase excursion is substantially larger or smaller than one radian. There is an equivalence between a shallow amplitude and a shallow phase screen.

CHAPTER II

EXPERIMENTAL INVESTIGATION

This study is concerned with certain aspects only of the design of the scanned antenna system. However, for convenience the entire system will be described.

A. APPARATUS

The primary considerations in the design of the wide aperture, high directivity, scanned antenna array are:

1. the overall antenna system must be capable of a rapid scan of all antenna elements and be suitable for use at long distances;

2. the system must provide a measure of the amplitude and phase of the signal at each antenna as well as the sense of the phase variations;

3. the amplitude and phase display must be readily convertible to digitisation for analysis by a high speed digital computer;

4. the system must be insensitive to local climatic variations.

The two elements of the scanned antenna system developed as part of this study are a semiconductor switch and a so-called "stairstep generator". These elements will be described first. In addition, a device was developed to adapt the switched antenna system for continuous recording of the phase of the received signal at all antennas.

The rapid scan of antenna elements is accomplished by the use of a semiconductor switch which was designed and developed as part of this study. The basic switch unit is shown in Figure 1. A bias voltage of approximately 10 volts is applied to R_3, which maintains diode D_2 in a state of conduction for the case when no positive voltage is applied to diode D_1. When a positive voltage is applied to D_1, the current across R_2 increases until the voltage drop there is sufficient to counter the voltage across R_3. At this point conduction of D_2 ceases. The resistive path defined by the series connection of D_1 and D_2 is thus seen to vary from a maximum to a minimum and then to a maximum. In effect this series path executes an "on-off" sequence equivalent to that of a conventional switch. For the "on" period a low impedance path exists for the signal from the antenna and preamplifier to the receiver.

When the first antenna is shut off due to the high impedance of D_2, because of the series arrangement of the switches as shown in Figure 2, switch unit number two begins the same "on-off" cycle. It should be noted that D_1 in the first unit maintains a low impedance path which, in conjunction with the low impedance of the diodes in unit two, again provides a path for antenna number two into the receiver. Similarly when D_1 in each unit is started into conduction, it maintains this conduction for continuously increasing positive voltages and provides a low impedance

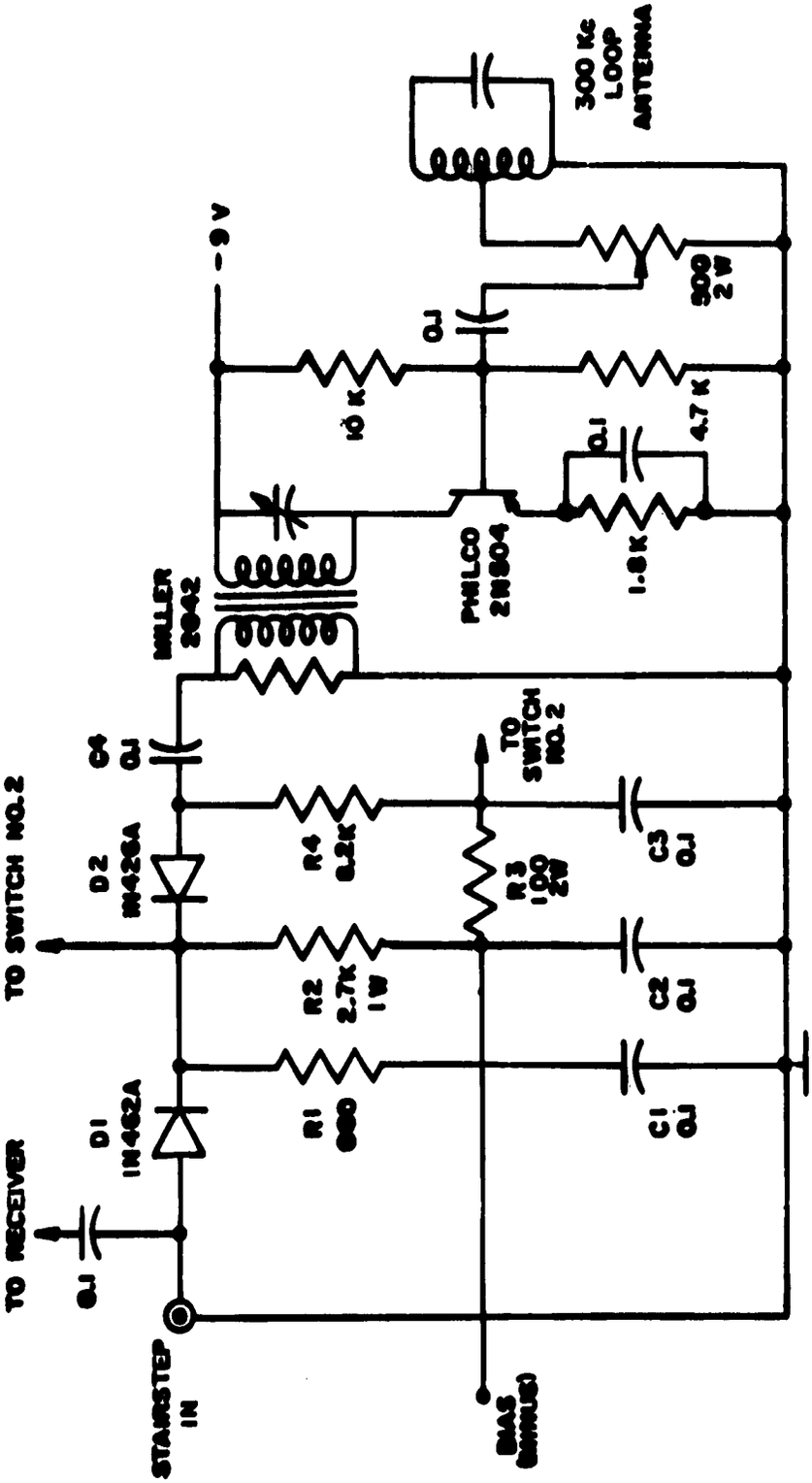

SEMICONDUCTOR SWITCH AND PREAMPLIFIER

FIGURE 1

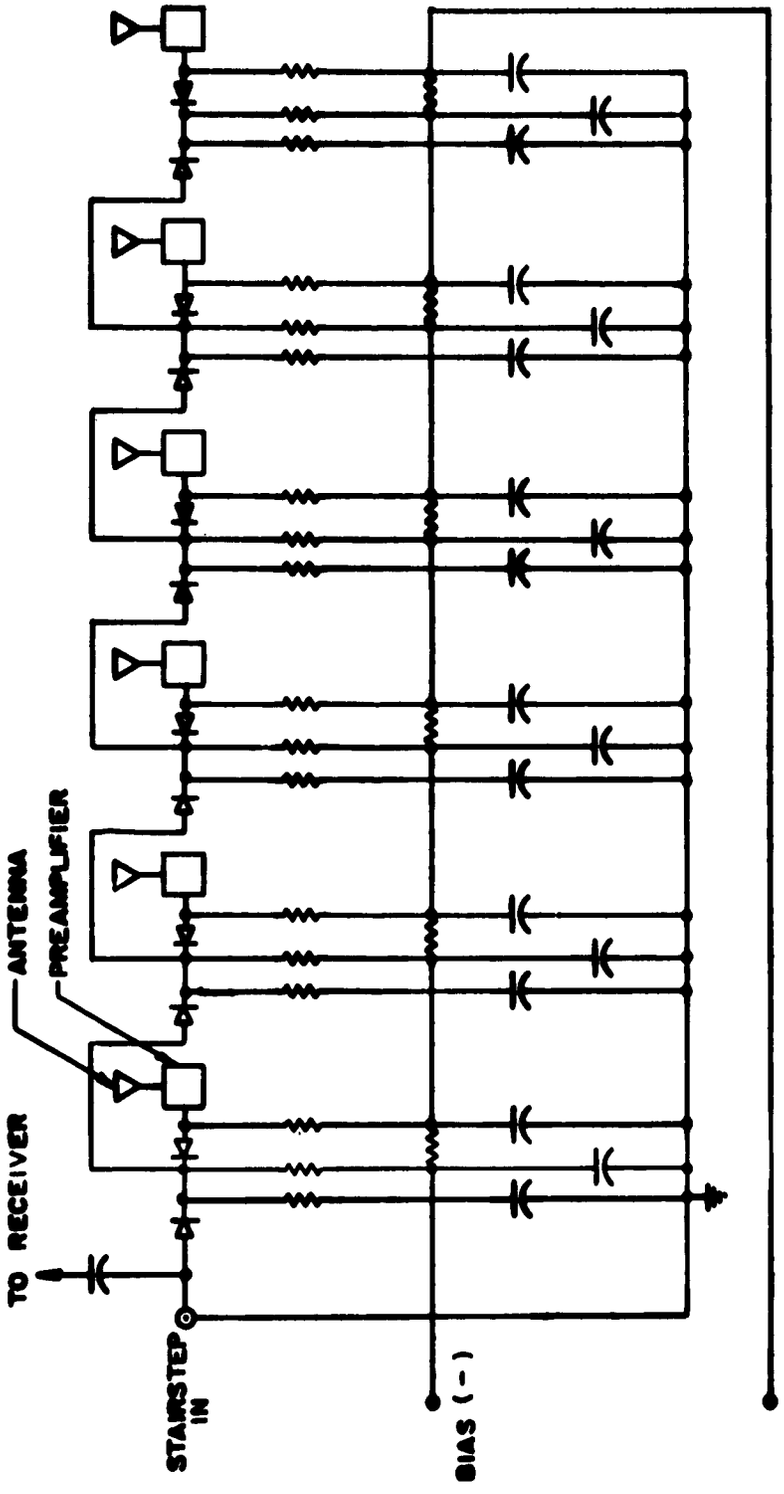

SERIES CONNECTION OF ANTENNA SWITCHES

FIGURE 2

path for subsequent switch cycles. Referring again to Figure 2, the switching operation entails six "on-off" arrangements using identical components and connected as shown.

The transistor preamplifier shown in Figure 1 serves two purposes. First it raises the received signal above the noise level encountered along the shielded feed lines; second it provides a ready means for adjusting the relative amplitudes of the received signals to allow for attenuation along the line and to allow for slight discrepancies in part selection.

If a positive voltage which increases continuously is applied to the semiconductor switch arrangement, each of the six antennas will be sequentially sampled individually. The only requirement is that the total switching voltage be larger than the total bias voltage. The first switching method that suggests itself, therefore, is a sawtooth voltage such as that which is available from the horizontal sweep circuits of oscilloscopes. This method was investigated, but it was found to have an inherent shortcoming. Since the gate operation of the switch does not describe an instantaneous "on-off" cycle with a constant impedance for the "on" time, minor changes in the repetition frequency of the received signal would change the position of the signal in the gate and change its amplitude independently of ionospheric changes. This shortcoming

results because the sawtooth voltage once started on one pulse of a train is insensitive to subsequent changes in the pulse spacing of the train.

A device was thus needed which would provide a constant voltage for a period of time sufficient to receive the pulse and which would be insensitive to minor variations of the pulse repetition frequency. This problem was solved by the design of a device named a "stairstep generator". The purpose of this device is to produce a succession of equal voltage steps each of which lasts the same period of time. Referring to Figure 3, the tubes V_1, V_2 and V_3 are trigger and delay circuits which provide the input to a Miller integrator, tube V_7, through the connecting diode V_4. The delay output is such that each step of the train exactly brackets the received signal in time. For the six antennas six steps are required. The recycling of the stairstep generator is accomplished by means of a delay gate linked to the oscilloscope sweep. At the end of each sweep the gate is applied to the cathode follower V_5 which in turn feeds the dual diode V_6. The action of the diode discharges the capacitor on the input of the Miller integrator V_7 and allows the unit to perform another cycle.

Although the semiconductor switching arrangement is the basic unit of the wide aperture, switched antenna system, there are associated units necessary for the recording scheme. A simplified diagram of the various units and

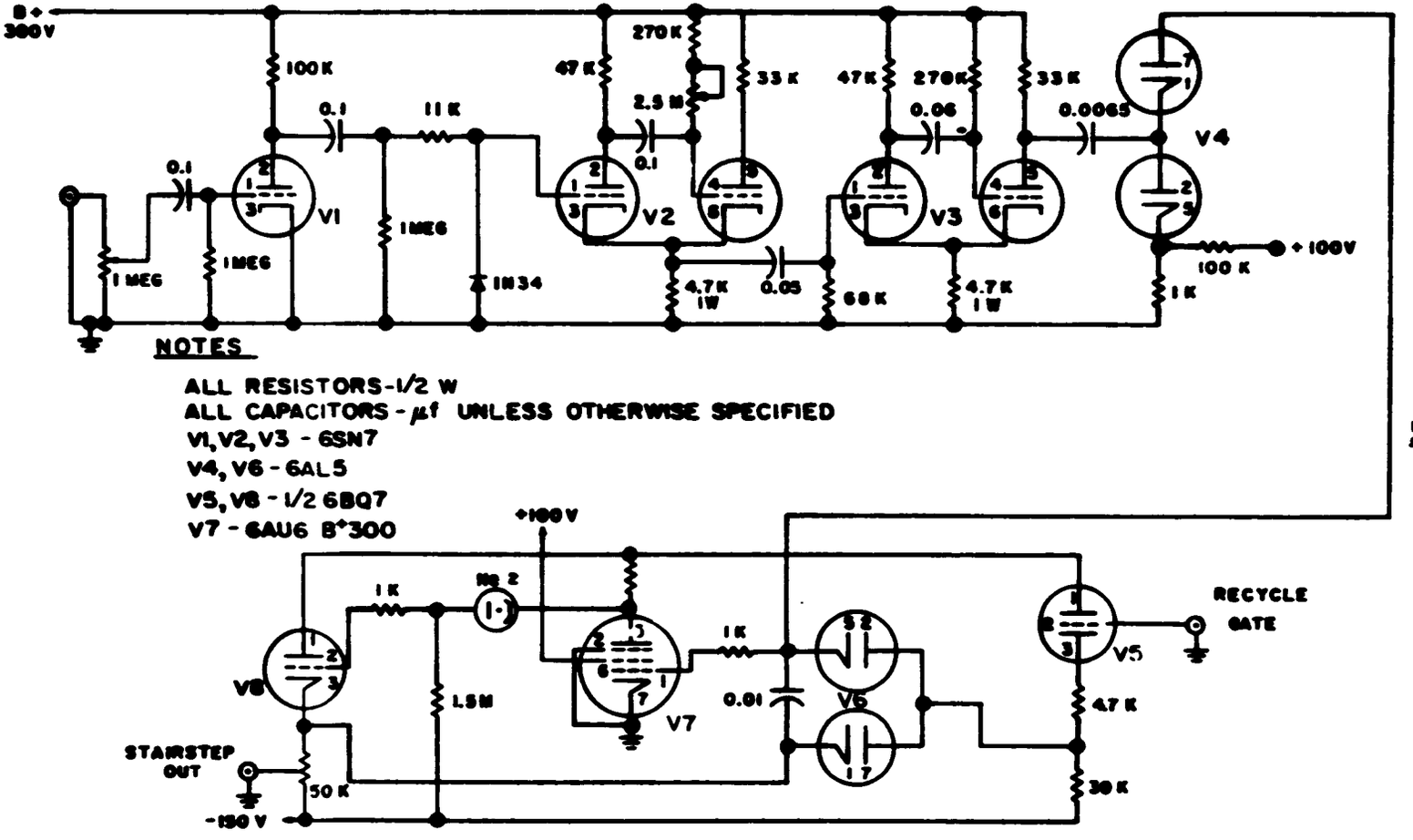

STAIRSTEP GENERATOR
FIGURE 3

their interdependence is shown in Figure 4.

The 27 mc/s receiver is the basic synchronisation unit of the antenna system. The 27 mc/s receiver output is a train of pulses with a pulse repetition frequency of 12/sec. The 300 kc/s pulse transmitter of the Ionosphere Research Laboratory, which is located at Scotia, is triggered by the same unit which produces the 27 mc/s synchronisation pulses. However, the synchronization pulses are transmitted approximately 50 microseconds before the 300 kc/s pulses so that the ground pulse and echo both appear at the beginning of an oscilloscope sweep. The phantastron unit, which is fed by the output of the synchronisation receiver, rejects spurious interference and noise from the 27 mc/s receiver output and provides a clean trigger for subsequent functions.

The stairstep generator has already been discussed; however, the unit marked "low impedance" at the output of the stairstep generator has not been discussed. It will be noted, however, that this unit supplies the stairstep impulses to the switched antenna. This impedance generator, designed by S. A. Bowhill of the Ionosphere Research Laboratory, is required for coupling because of the relatively high currents used in switching. It also supplies a ready means of adjusting the stairstep level so that the voltage is sufficient to operate all of the units of the switched antenna system.

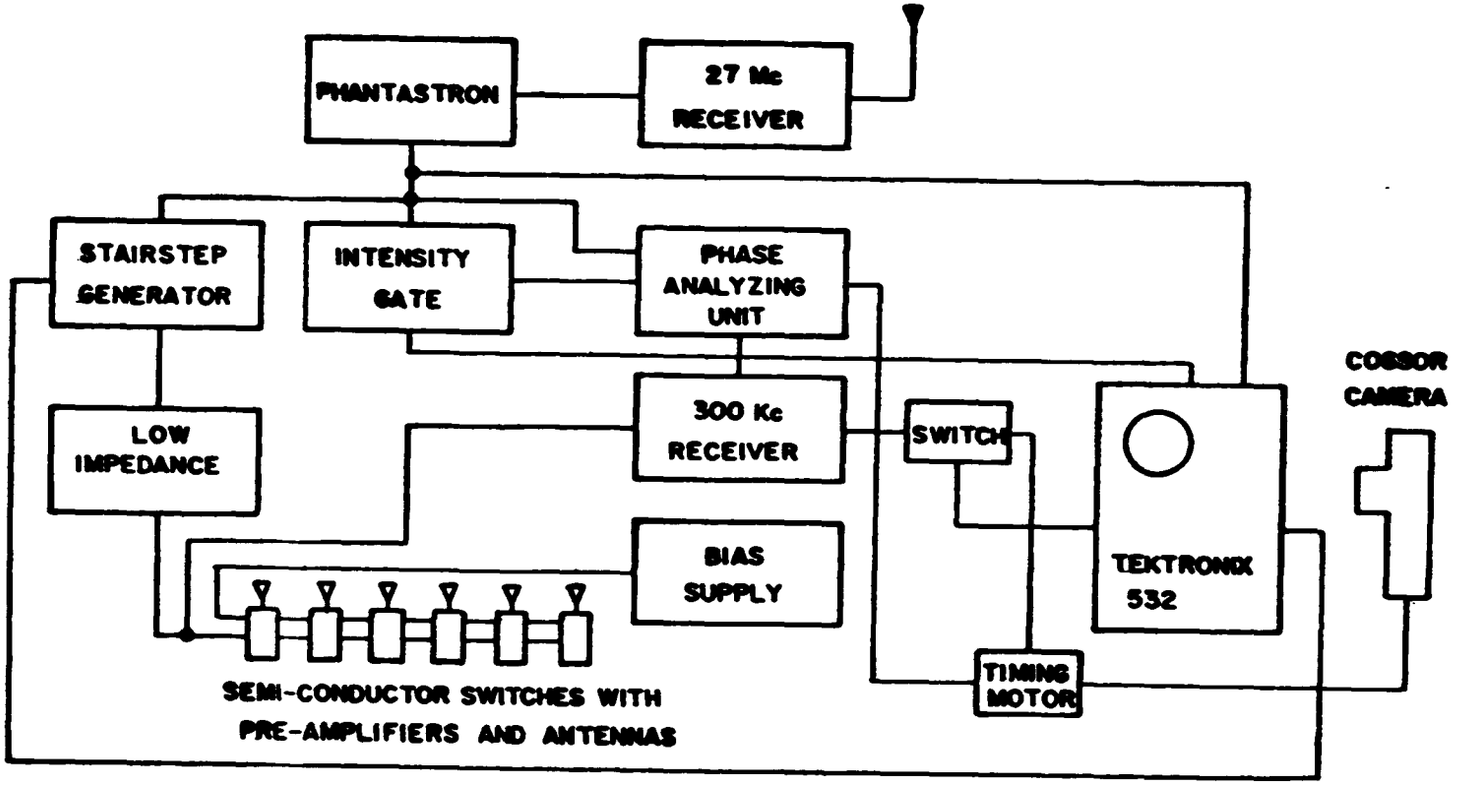

WIDE APERTURE SWITCHED ANTENNA SYSTEM

FIGURE 4

If multiple echoes are present after reflection from the ionosphere, a method must be available for rejection of the unwanted ones before photographing. The intensity gate provides such a method. It consists of delay multivibrators which provide a 300 μsec pulse to be applied to the cathode of the recording oscilloscope at the time the echo appears. By reducing the intensity of the oscilloscope, only the selected echo is visible for photographing. This brightening gate also has an application in the phase analyzing unit to be discussed in a subsequent section of this chapter.

The 300 kc/s receiver employed in the switched antenna system was designed by P. A. Chiavacci of the Ionosphere Research Laboratory. It is a superheterodyne receiver employing three radio frequency stages at 300 kc/s and a mixer and three intermediate stages at 1400 kc/s.

The bias supply is a Lambda power supply model 71, which delivers approximately 50 ma at 30 volts under normal operating conditions. It has a vernier on the voltage adjustment for minor changes of the switch operating voltages.

The timing center is a 20 rpm motor which operates a microswitch. This in turn supplies the necessary impulses to advance the film and switch the sampling from amplitude to phase at the unit labeled "switch". The recording camera is a Cossor camera modified by the addition of a pulse motor on the film advance shaft. This allows a snapshot form of

recording. Since the recorded signal voltages vary sometimes very rapidly, a small horizontal shift is imposed on the oscilloscope trace as the film is advanced. At the next film advance the trace returns to its original position and the cycle then repeats. This prevents the recorded signals from running into each other.

The method of operating the equipment and measuring amplitude variations at the antennas as a function of time will now be described. With all units turned on, the bias voltage should be adjusted to 30 volts. A fluctuation of the current indicator on the bias supply of approximately $\pm$ 5 ma about the 50 ma mark indicates that the stairstep generator is coupled into the line. The period of fluctuation of the meter is that of the oscilloscope sweep which is 500 m sec. The stairstep output may be monitored at the output of the low impedance unit by a test jack at the front of the unit. The gain adjustment of this unit, also located on the front of the chassis, should be adjusted so that the stairstep output is about 5 volts per step. The delay gate control on the oscilloscope should then be adjusted so that the stairstep recycles after six steps.

At this point the output of the receiver can be monitored. With maximum receiver gain the noise output appears as six discrete portions corresponding to the six antennas. If, at this time, a 300 kc/s CW signal is applied

to the positive bias wire shown in Figure 2, it serves as an antenna; and the receiver output now consists of six impulses of varying height each as wide as the "on" time of a single step.

The system is now ready for recording. After turning the CW signal off, the oscilloscope sweep period is decreased so that one ground pulse and the sky waves can be observed. An integral part of the low impedance generator is a variable voltage which can be used to sample any of the antennas. Usually it is set to sample antenna number 1 at this time, and the intensity gate is adjusted so that only the selected echo is visible when the intensity is turned down on the oscilloscope. When this is done, the sweep rate is returned to 500 m sec, and the low impedance generator is switched to couple the stairstep to the switches.

Across the face of the scope six impulses should appear which correspond to the signal amplitudes at the six antennas. The timer unit is then activated, and a recording is made of the time variations at each antenna. Normally the records of the first night are used to adjust the individual preamplifiers. By averaging the outputs at each antenna for a long period of time the correction factors necessary to equalize the individual gains are obtained. These corrections can be made readily by means of the gain control on each preamplifier. Normally one such adjustment

is satisfactory for the life of the battery in each unit. Operation periods of two months and longer have been used with good results. A typical field antenna unit is shown in Figure 5.

B. PHASE ANALYZING SECTION OF THE SWITCHED ANTENNA SYSTEM

The method of detection of phase variations with the wide aperture, switched antenna system is similar to that employed by Houston.[16] In this method the voltage of an oscillator is phase locked to the ground pulse at a frequency lower than that of the echo. The echo is then mixed with this oscillation, and the phase changes appear as interference fringes which are displaced in time with changing phase of the observed sky wave. This method is equivalent, for example, to the use of two closely spaced wavelengths of light in a Fabry-Perot interferometer.

The fringe display method is unsuitable for use in the switched antenna system because of the requirement that the display be readily adaptable to digitization. An alternative method is to phase lock a burst of oscillation at the same frequency as the echo. When the echo is mixed with this burst, phase changes will appear as changes in amplitude about the level of the locked oscillator.

The method of phase detection is shown in Figure 6. The amplifier and blocking oscillator are fed by the phantastron output and supply the trigger for a delay multivibrator. The delay is necessary because the

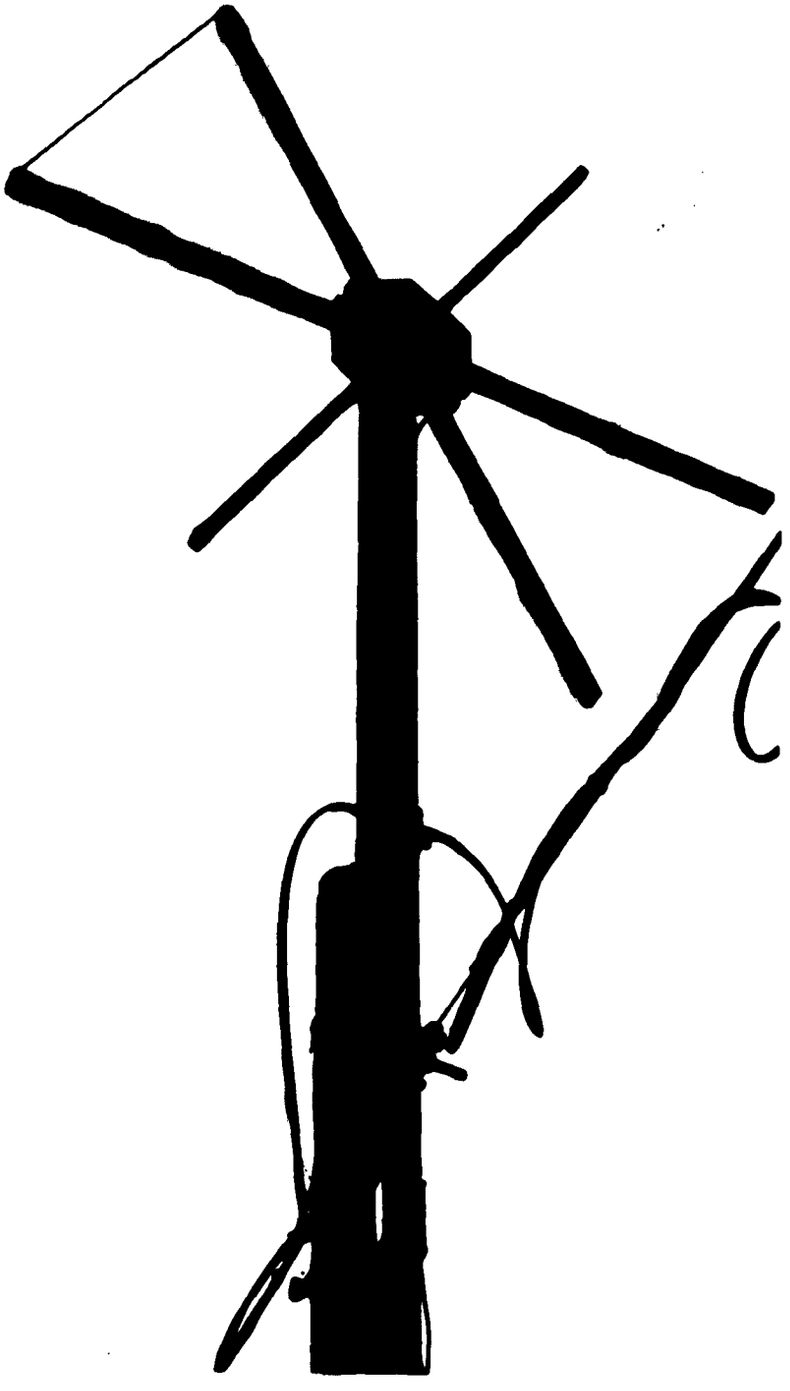

TYPICAL ANTENNA UNIT

FIGURE 5

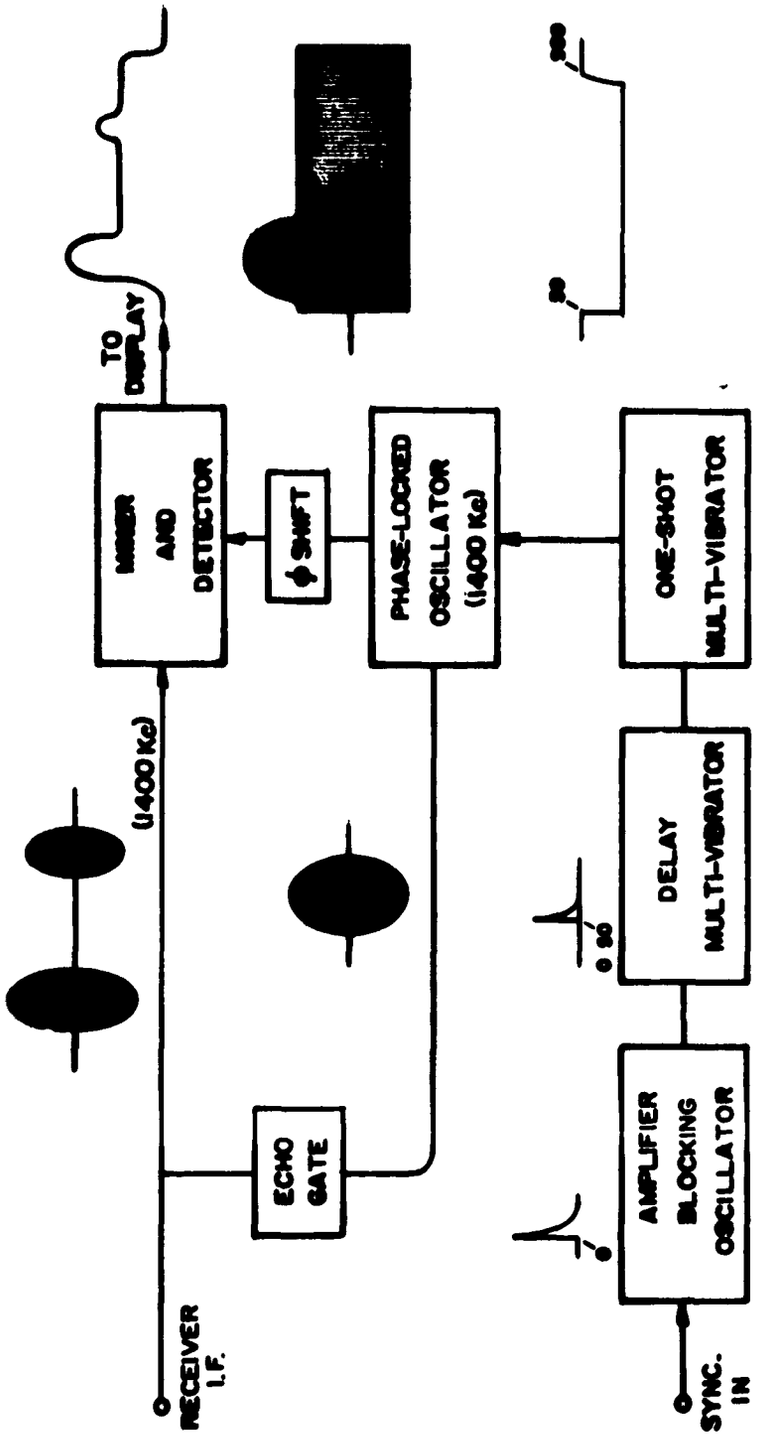

BLOCK DIAGRAM OF PHASE ANALYZING METHOD

FIGURE 6

synchronisation pulse leads the ground pulse by approximately 50 μsec. The one-shot multivibrator has a negative output pulse, 900 μsec long which gates a 1400 kc/s oscillator. The output of the superheterodyne receiver is applied to two places. First the echo is gated by the intensity gate pulse previously described, so that only the ground pulse phase locks the triggered oscillator. If the gate were not used, when the echo gets large it would also phase lock the oscillator and defeat the purpose of the experiment. The ground pulse and echo are then mixed with the phase locked oscillator and detected. To provide a measure of the sine and cosine of the phase angle a 90 degree phase shift network is activated on alternate scans of the antenna system. This serves to indicate the sense of phase variations and provides a measure of the relative phase angle. The theory of its operation will be discussed in Chapter III.

The detected output pictured in Figure 6 shows an "in phase" condition for the echo. As the phase of the echo changes through 180 degrees, the echo will appear as a subtraction from the fixed level of the detected oscillator output.

The recording sequence for one complete sample of the complex amplitudes of the antennas is: amplitude, phase (phase shifter out), amplitude and phase (phase shifter in). The timing unit and switch shown in Figure 4

accomplish this sequence.

A schematic of the phase analyzing unit is shown in Figure 7. Tube V_4 is the amplifier and blocking oscillator which triggers the delay multivibrator V_5. The delay multivibrator subsequently triggers the one-shot multivibrator V_6. The phase coherent oscillator consists of V_2 and V_7. This is a cathode coupled negative resistance circuit which controls the tuned circuit T_4. The tank circuit T_4 is essentially short-circuited when V_7 is in the rest position. This tube V_7 acts as a gate which is unclamped by a negative signal from V_6.

The secondary of T_4 is centertapped and provides two signals 90 degrees out of phase. These two signals are applied to the grids of the identical cathode followers of V_3, and the outputs are alternately sampled for mixing with the echo. The 90 degree phase shift is checked by sampling both outputs on a dual-channel oscilloscope.

The IF signal is fed to V_1 on the screen grid, and the intensity gate, a negative pulse, is fed to the control grid for echo suppression. The output of V_1 is then used to phase lock the oscillator. The mixing of the phase locked oscillator and the echo takes place in tube V_8.

All normal adjustments of the phase analyzing unit can be made by controls located on the front panel of the unit. Preparation for recording is accomplished by

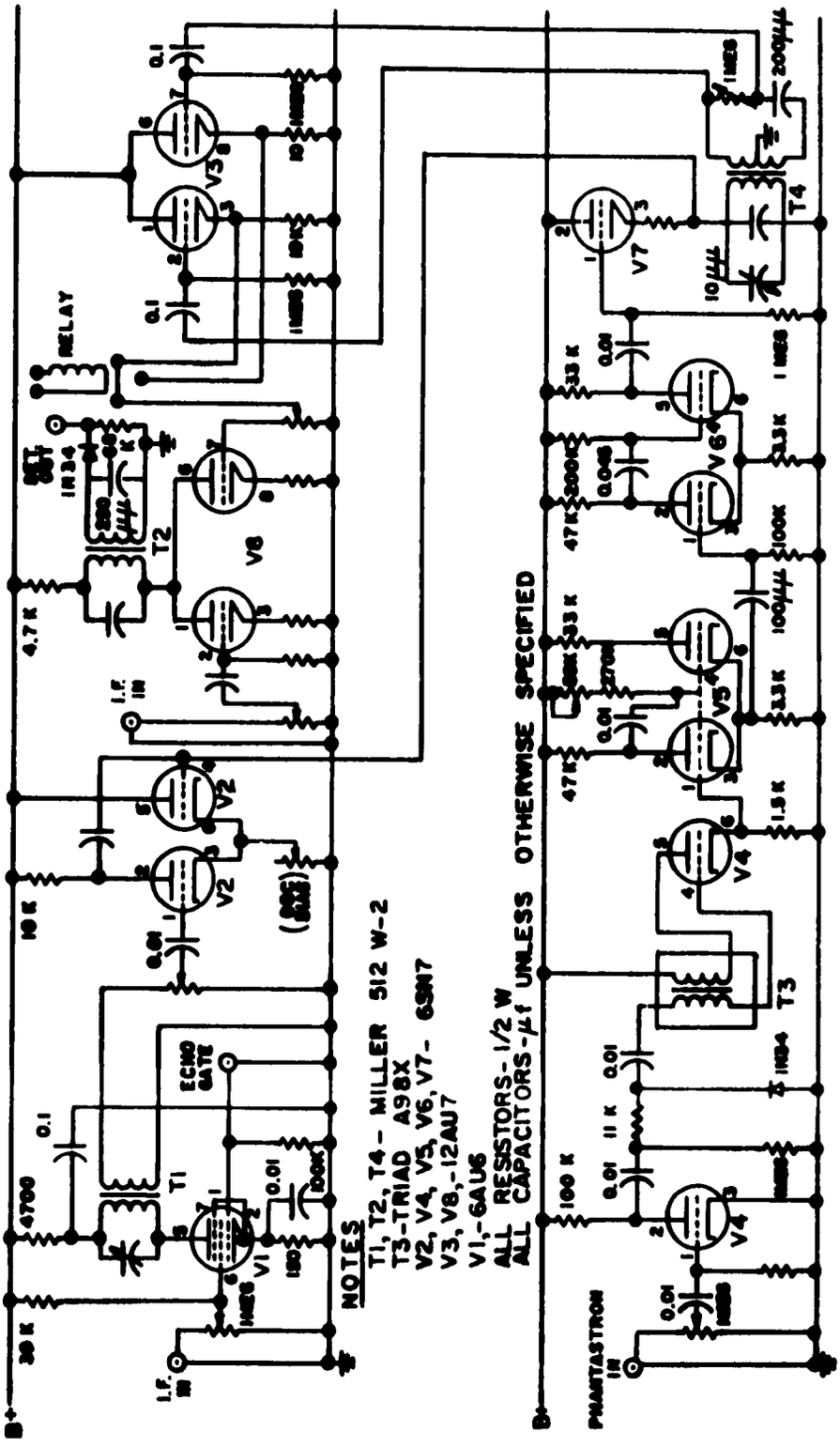

PHASE ANALYZING UNIT

FIGURE 7

visual monitoring of the phase unit output on the recording oscilloscope. The position of the phantastron input control is such that the blocking oscillator is just triggered. The amplitude of the local oscillator is adjusted so that the detected output as shown on Figure 6 is about 5 volts. The local oscillator frequency is adjusted at T_4 so that the echo appearing on the detected output has a Gaussian envelope without interference fringes of the kind described above. Slight variations in frequency about the center frequency of 1400 kc/s then cause the echo to undergo an apparent phase shift of 180 degrees or cause the detected output to reverse in sign.

The level of IF signal necessary to phase lock the oscillator can be determined as follows. As the IF level is reduced, the detected ground pulse suddenly starts to change amplitude in a random manner, indicating loss of phase lock. An alternative method is to remove tube V_1. This removes the phase locking signal, and fluctuations take place corresponding to the difference in complex voltage between the oscillator and the ground pulse.

Under correct operating conditions the ground pulse, being the phase reference, appears as a steady signal imposed on the pulsed oscillator. The echo, on the other hand, undergoes gradual changes from positive to negative and back as the phase path of the sky wave changes.

Comparing the original specifications of the

switched antenna system with the working system it is found that all requirements stated at the beginning of the chapter have been met. First a rapid scan is achieved by means of the semiconductor switch arrangement; in fact, all antennas are scanned in 0.5 sec. The system operates with a spacing of 180 feet between antennas and, including supplementary feed cables, extends about 1600 feet overall. A portion of the antenna is illustrated in Figure 8. In further work a line of six antennas was constructed with a spacing of 900 feet between antennas, covering a total distance of about 7000 feet including supplementary feed cables. This fulfills the requirement that the system should operate with wide aperture. A measure of the amplitude and phase at each antenna, as well as the sense of the phase variations, has been provided. Moreover, the method of detection is readily adaptable to digitization. All components of the system are relatively insensitive to climatic variations. The switching diodes are silicon and not subject to variation with temperature over the local range which has been encountered. The preamplifiers have demonstrated the ability to operate for long periods in all seasons with minimum maintenance.

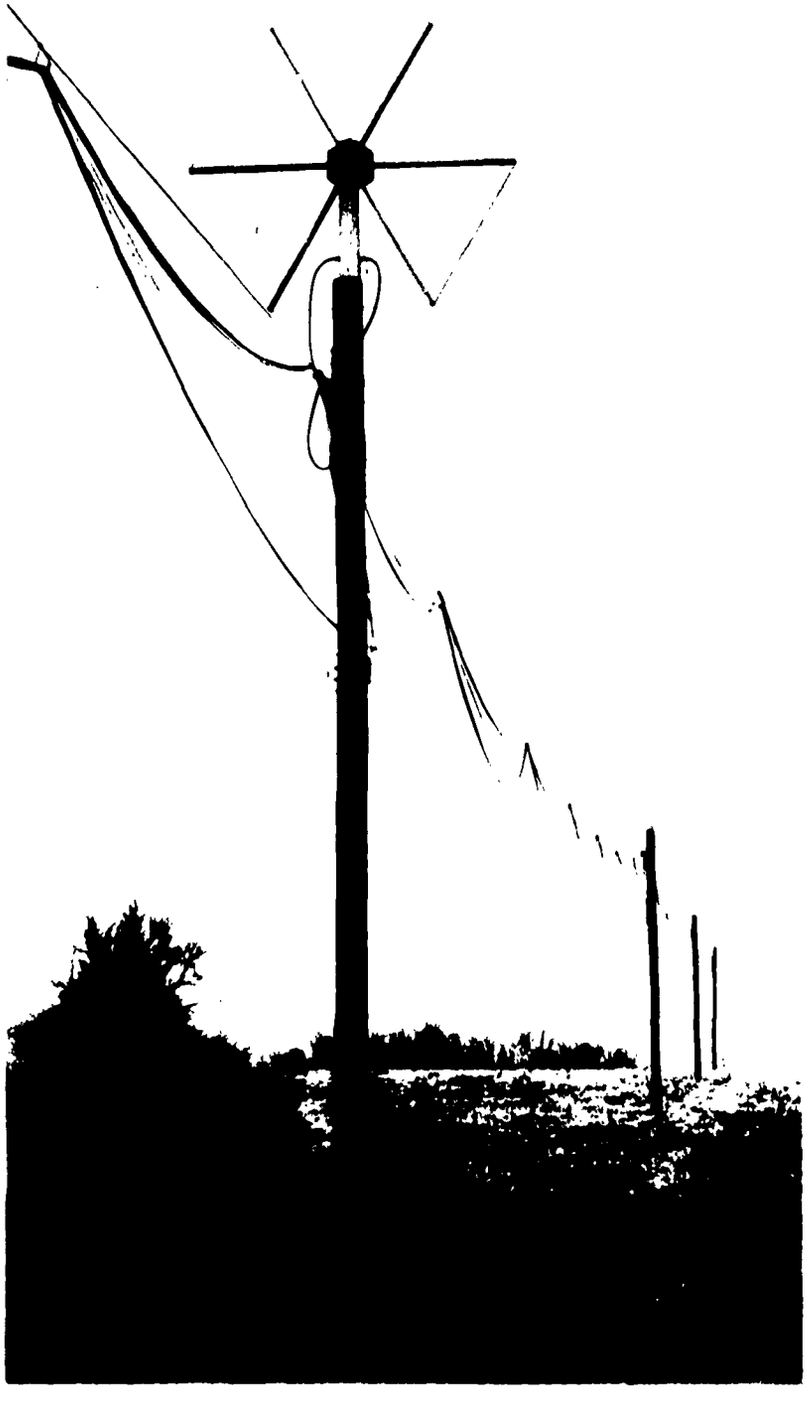

SECTION OF SWITCHED ANTENNA-ARRAY

FIGURE 8

CHAPTER III

EXPERIMENTAL RESULTS

A. REDUCTION OF RECORDS

A typical section of record taken with the wide aperture antenna system is shown in Figure 9. In successive intervals of three seconds the following parameters are measured: amplitude, in-phase component, amplitude and quadrature component. The time for each sample could be shortened by a factor of three, but the fade periods are easily observable with a three second sample, and the extra time for photographic integration gives superior records.

The analysis of the amplitude portions of the record proceeds as follows. Using a 35 mm desk projector, the pulse lengths are measured with a scale suitable to cover the range of amplitude fluctuations over the sample time. The amplitudes are then plotted as a function of time for each antenna, as shown in Figure 10. In this diagram the various amplitudes have not been normalized. That is, no compensation has yet been made for preamplifier gain differences and line attenuation.

It is apparent from comparison between the amplitude variations at each antenna that there is a high degree of correlation between close antennas and that the correlation decreases with increasing separation of the antennas being compared. Since the various maxima and minima are related, if the antenna array were planar instead of linear,

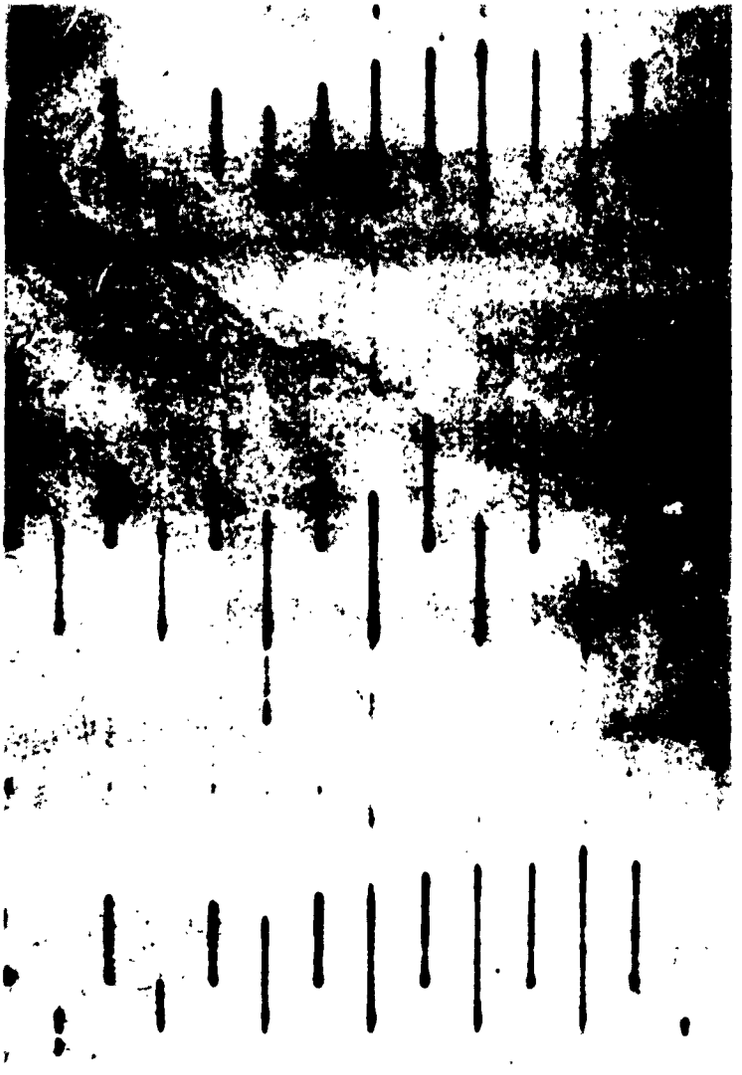

TYPICAL SWITCHED ANTENNA RECORD

FIGURE 9

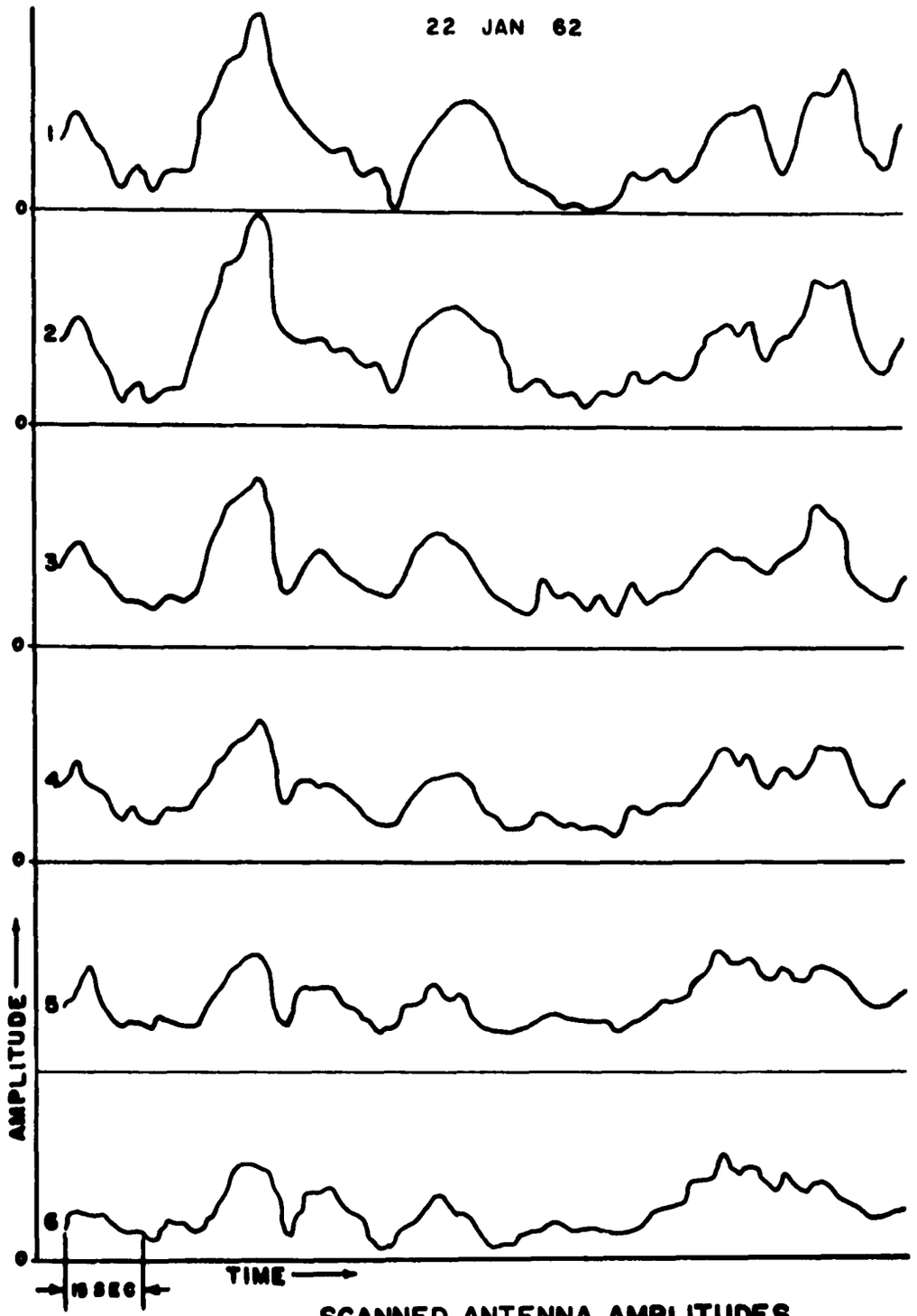

SCANNED ANTENNA AMPLITUDES

FIGURE 10

a measure of the temporal displacement of related fluctuations would give the drift velocity of the irregularities causing the fluctuations.

The scaling of the phase records is also simple. A reference line was provided on the oscilloscope display which appears as a white spot on the film. The magnitude of the excursion of the display from this reference gives a measure of the in-phase and quadrature phase components.

For each antenna it is necessary to measure the pulse height and its sense for the two cases when the phase shift network is active and inactive. Since the phase shift activation increases the phase of the sky wave by 90 degrees, the phase angle at each antenna can be determined by the following procedure.

Assume that the phase excursion when the phase shift network is inactive, given by

$$A_o = R \sin\phi, \tag{1}$$

where R is some constant or function of the adding circuit. Then since

$$\sin(\phi+90^o) = \cos\phi, \tag{2}$$

if A_1 indicates the phase excursion with the phase shifter in then

$$\frac{A_o}{A_1} = \frac{R \sin\phi}{R \cos\phi} = \tan\phi; \tag{3}$$

or, conversely, the phase angle is given by

$$\phi = \arctan \frac{A_o}{A_1}. \qquad (4)$$

The ratio of the two phase components is thus a measure of the phase angle of the received wave. The quadrant in which the angle lies can be determined from the sense of the phase components. For example, if the introduction of the phase shift results in a positive signal as previously defined and if the original signal was positive, then the angle lies in the first quadrant since the phase shift is a lead. Similarly, a change from positive to negative indicates the second quadrant, negative to negative the third and negative to positive the fourth quadrant.

The results of this analysis are shown in Figures 11 and 12 for the phase records taken with the amplitude records of Figure 10. The time scales for the phase and amplitude variations are the same.

B. THE WIDE APERTURE ANTENNA AS A DIRECTION FINDER

A detailed statistical study of records obtained with the wide aperture antenna system is beyond the scope of this study; however, if the antenna system is treated as a phase sensitive direction finder, the angle of arrival of a specularly reflected wave can be determined. From geometrical considerations the angle of arrival should be 2 degrees from the vertical.

A phase sensitive direction finder compares the phase of two or more signals at antennas located a known

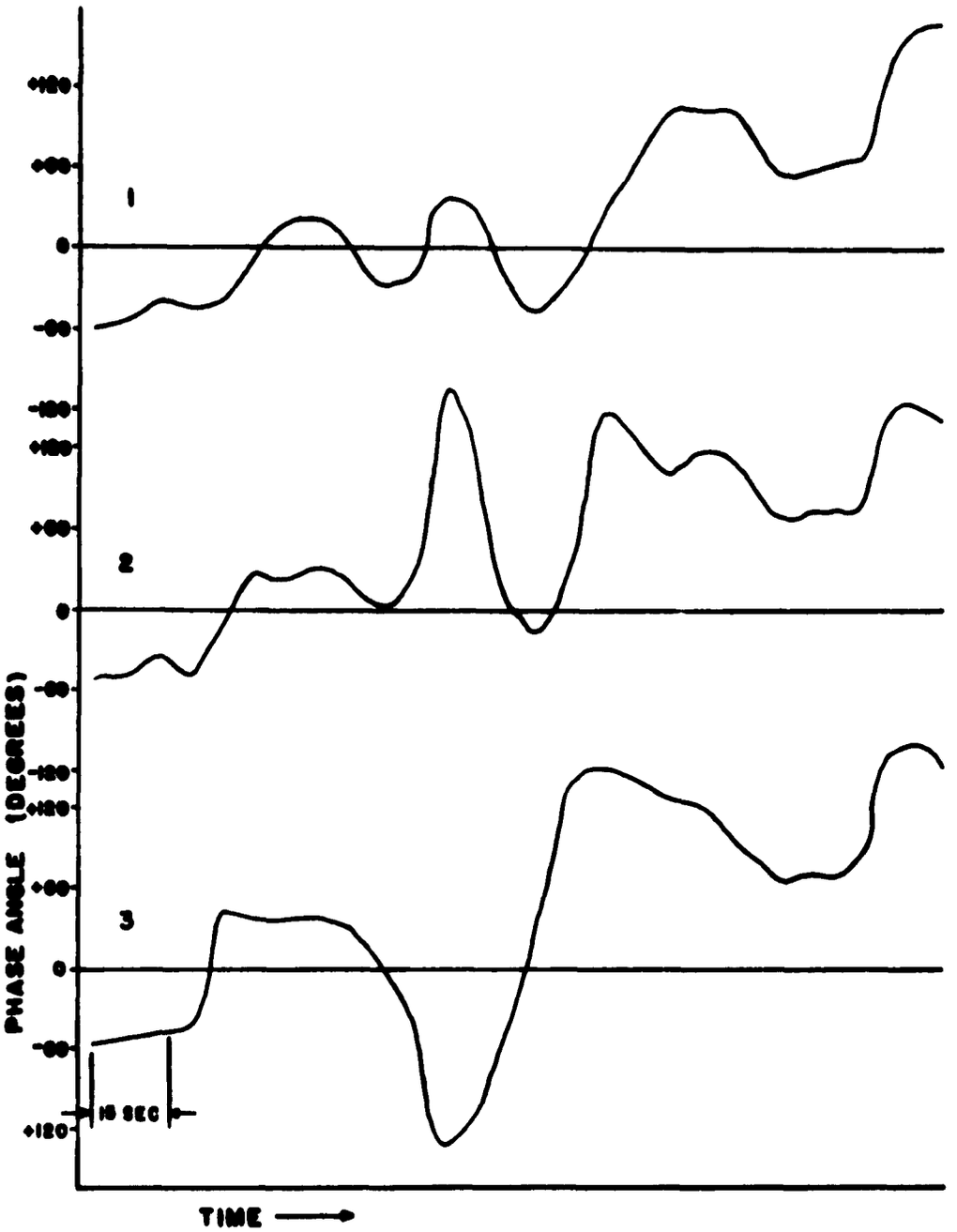

SCANNED ANTENNA PHASE VARIATIONS

FIGURE 11

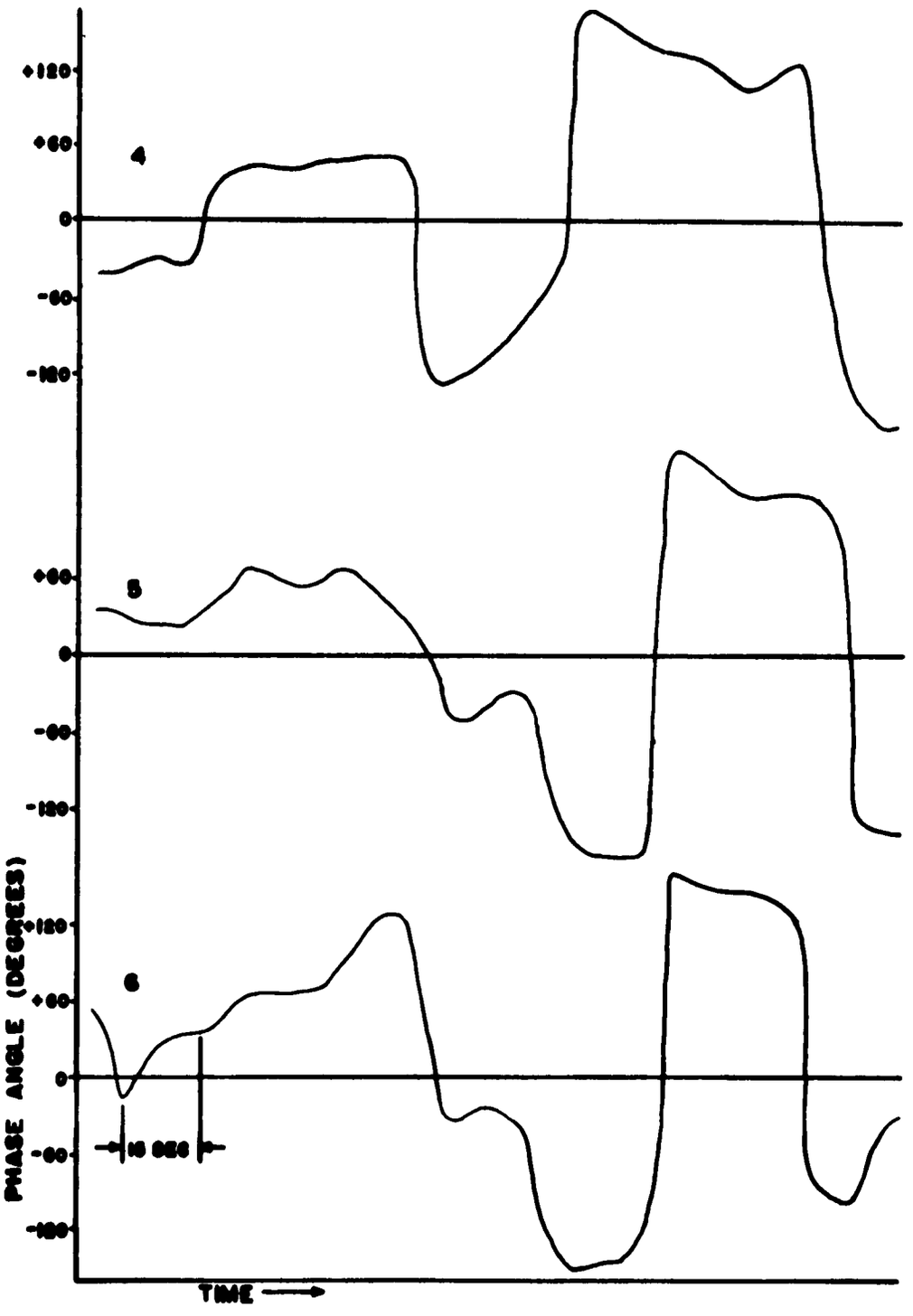

SCANNED ANTENNA PHASE VARIATIONS

FIGURE 12

distance apart. For an ionospherically reflected wave angles of arrival different from the vertical will cause a phase shift at each antenna relative to the first antenna. The magnitude and sense of the relative phase shift depends on the magnitude and sense of the angle of arrival.

The geometry of the transmitter and switched antenna locations is shown in Figure 13. The half-wave folded dipole at Scotia radiates the ground wave with a magnetic field wave normal inclined 28 degrees to the direction of the switched antenna array. Since the transmitter is located 5.5 km from the switched antenna and the height of reflection of the wave is approximately 100 km, the reference angle for specular reflection is 2 degrees from the vertical.

If the angle of arrival of the sky wave is denoted by θ_s, and ϕ_{1s} and ϕ_{2s} are the phase angles, respectively, of the first and last antenna in the line, then

$$\phi_{2s} - \phi_{1s} = \frac{2\pi d}{\lambda} \cos\theta, \qquad (5)$$

where d is the separation distance of the two antennas, and λ is the wavelength. Similarly if θ_g is the angle of arrival of the ground wave and ϕ_{1g} and ϕ_{2g} are the relative phase angles at the first and last antennas due to the ground wave, then

$$\phi_{2g} - \phi_{1g} = \frac{2\pi d}{\lambda} \cos\theta_g. \qquad (6)$$

Subtracting (6) from (5),

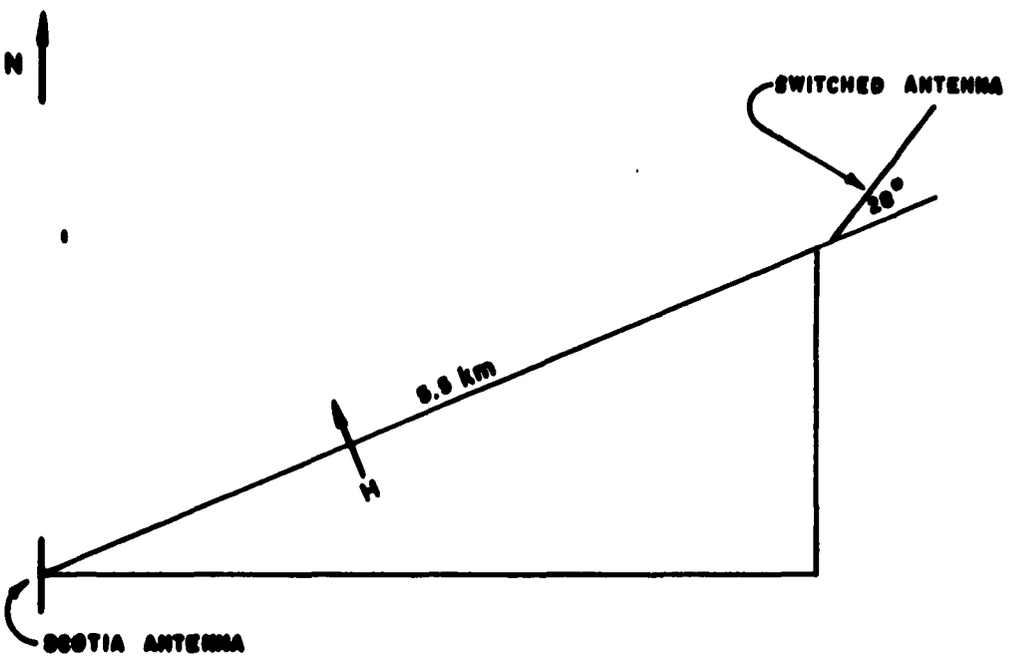

TRANSMITTER AND SWITCHED ANTENNA GEOMETRY

FIGURE 13

$$(\phi_{2s}-\phi_{2g})-(\phi_{1s}-\phi_{1g}) = \frac{2\pi d}{\lambda}\left[\cos\theta_s-\cos\theta_g\right] . \qquad (7)$$

The difference of the two quantities on the left side of equation (6) can be readily determined by the measurement of the relative phase difference along the line for echoes received from a quiet ionosphere. The records chosen are shown in Figures 14, 15 and 16. Aside from two marked deviations, the first portion of the amplitude record for antenna one and subsequent antennas shows a fairly shallow fluctuation with time. The relative phase differences along the line were calculated for this period, and the results are shown in Figure 17. The beginning of this time plot corresponds to the beginning of the amplitude and phase plots, and the time scale is the same. Since this phase difference ranges from zero to 10 degrees, if this is substituted in the left hand side of equation (7), the angle of arrival of the sky wave must vary from 49 degrees to 59 degrees from the vertical. For this computation λ is 1 km, d is 0.275 km and θ_g is 62 degrees.

The angle of arrival as computed from (7) is much greater than the expected value of approximately 2 degrees. This may be due to false assumptions about the specular reflection of the sky wave. The fault, however, appears to lie with an anomalous propagation of the ground wave. Tests have been made to determine the angle of arrival of the ground wave at each antenna, and it was found that

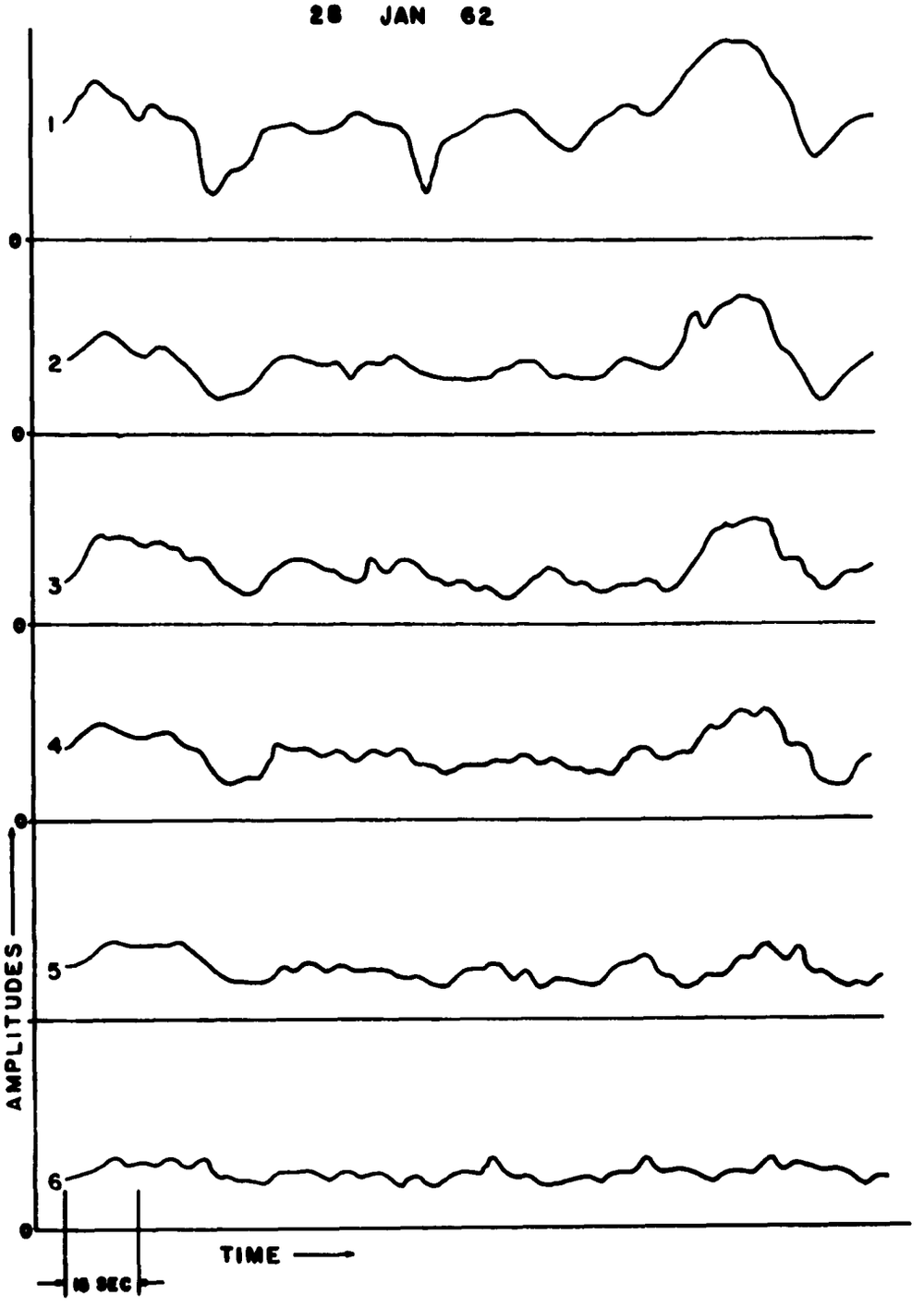

SCANNED ANTENNA AMPLITUDES

FIGURE 14

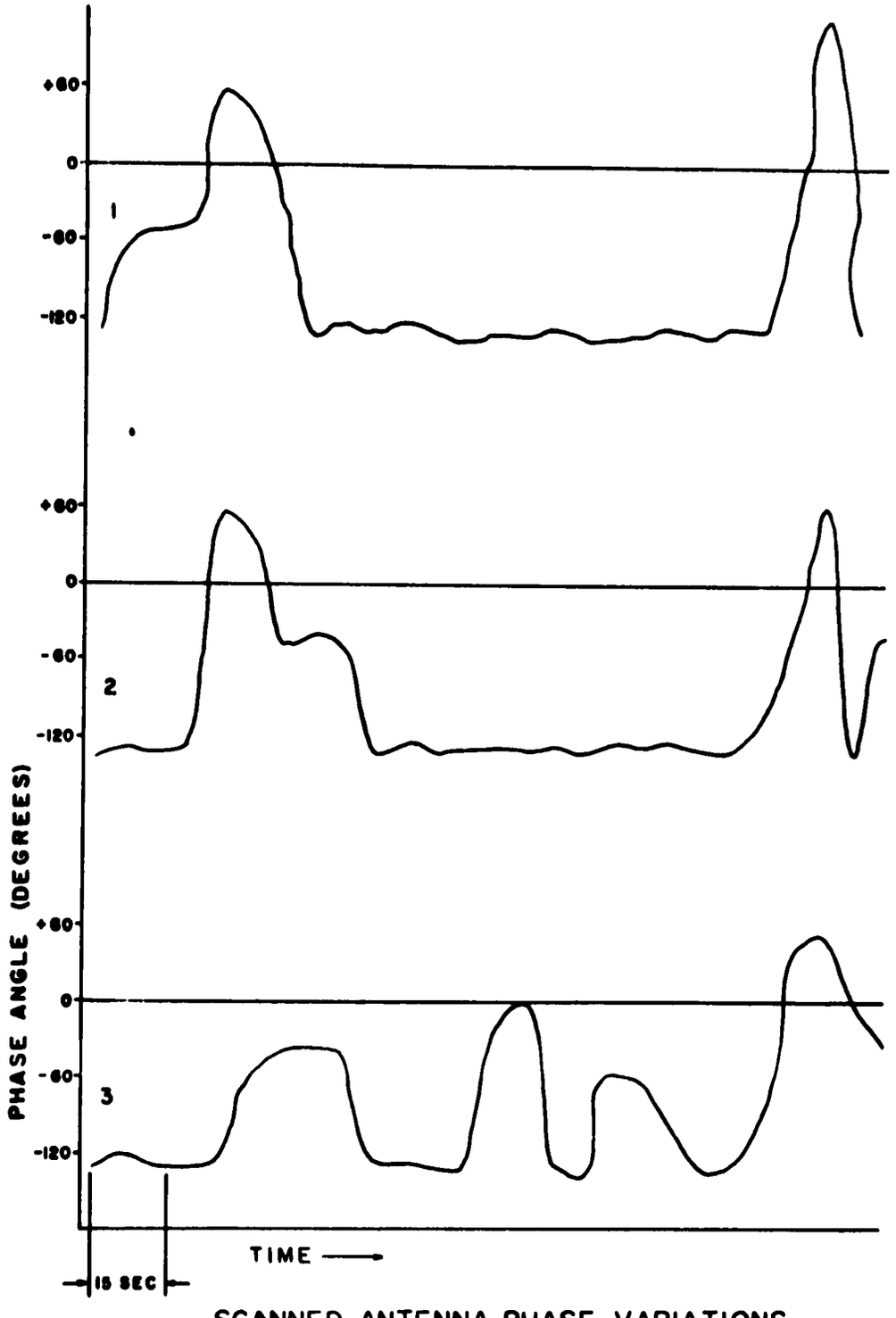

SCANNED ANTENNA PHASE VARIATIONS

FIGURE 15

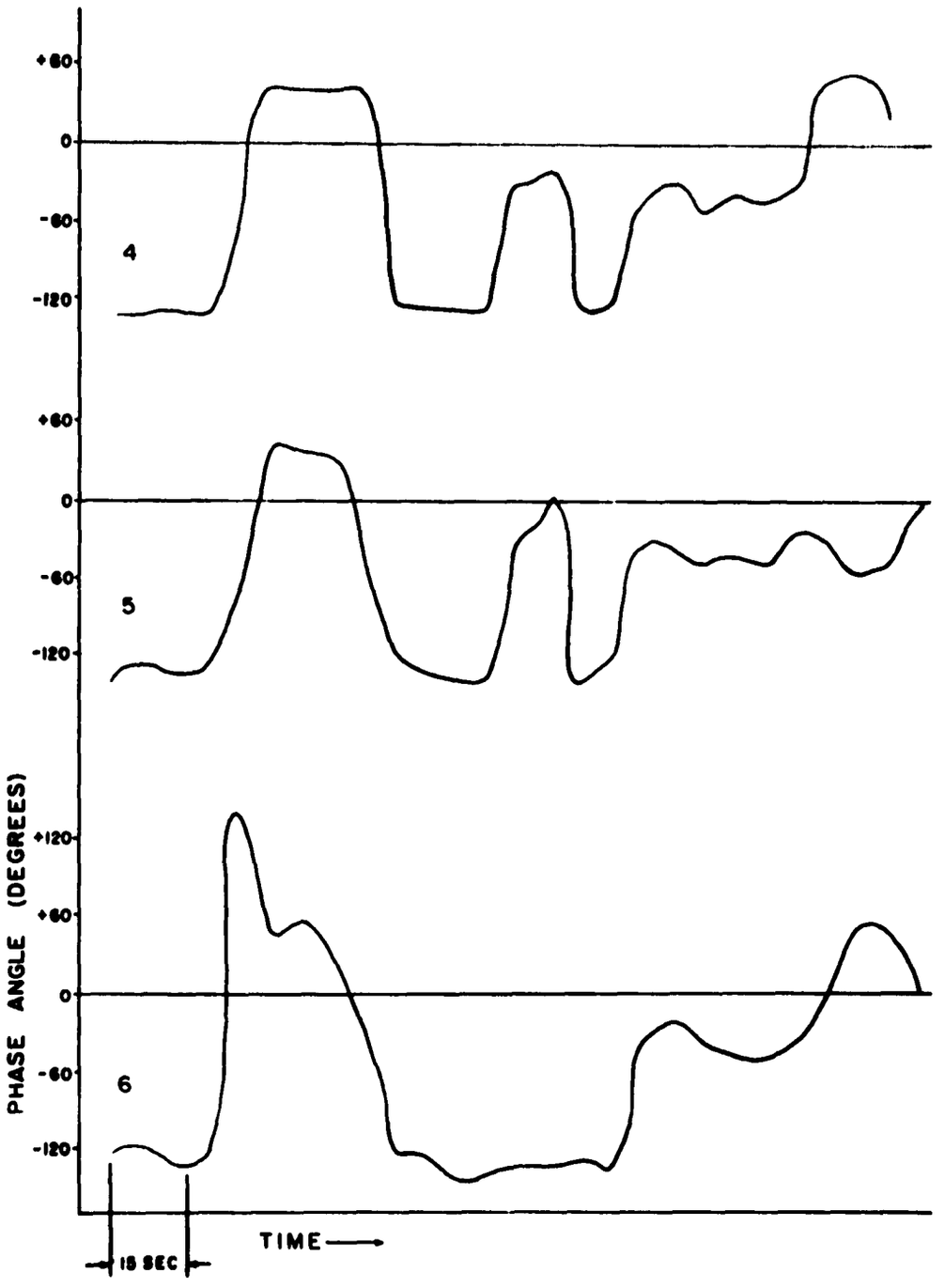

SCANNED ANTENNA PHASE VARIATIONS

FIGURE 18

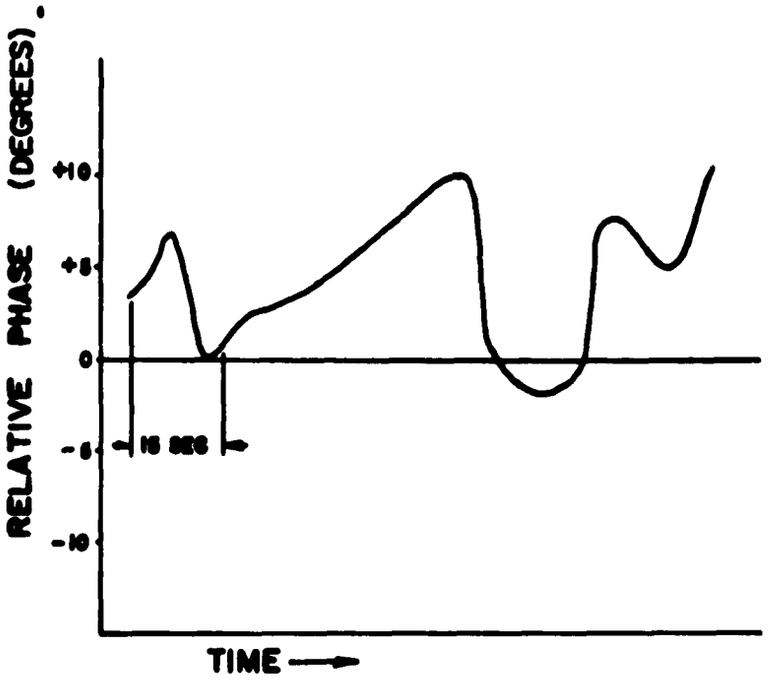

VARIATION OF RELATIVE PHASE WITH TIME

FIGURE 17

generally the angle of arrival was different at different heights on the supporting poles. In particular, the catenary supporting the necessary bias and shielded cables appears to affect the angle of arrival greatly. A method of overcoming this deficiency will be discussed in Section A of Chapter V.

C. COMPARISON OF RESULTS WITH OTHER WORK

If the angular spread of phase differences of the sky wave measured at the switched antenna array is treated as an angular spectrum, a comparison of the structure size of the irregularity causing the spread can be made with previous measurements at the same frequency.

Bowhill[14] showed that the angular power spectrum emerging from an irregularity is given by

$$W_n(s) \propto \exp\left\{-\frac{2\pi^2 D^2 S^2}{\lambda^2}\right\}, \tag{8}$$

where D is the structure size, and S is the sine of the angle between the wave normal and the vertical. For a Gaussian autocorrelation function the size of an irregularity is specified when the Gaussian drops to 0.61 or

$$\frac{2\pi^2 D^2 S^2}{\lambda^2} = \tfrac{1}{2}. \tag{9}$$

This gives a value of D,

$$D = \frac{\lambda}{2\pi S}. \tag{10}$$

The average angular deviation for the period shown in

Figure 17 is approximately 5 degrees. If D is computed from (10) where λ = 1 km and S = $\sin 5^{\circ}$, then D is 1.8 km.

Lee[22] in a separate measurement of structure sizes at 300 kc/s has found initially that the structure size is 3 $\pm$ 1 km. The result determined by the wide aperture switched antenna system is compatible with his findings. Further work is necessary, of course, in obtaining and reducing records before full credence can be placed in the results of the above analysis.

CHAPTER IV

THEORETICAL CONSIDERATIONS AND DISCUSSION

A. RAY THEORY

As a first method in the investigation of effects produced by an irregularity on incident radiation, geometrical optics will be employed. By definition this branch of optics is characterised by neglect of wavelength or is a treatment of propagating electromagnetic disturbances as rays not subject to scattering or spreading.

This limiting case of optics may be treated in terms of the first order Maxwell equations. In regions free of charges and currents these are:

$$\text{curl } H + ik_o \varepsilon E = 0, \tag{11}$$

$$\text{curl } E - ik_o \mu h = 0, \tag{12}$$

$$\text{div } \varepsilon E = 0, \tag{13}$$

$$\text{div } \mu H = 0. \tag{14}$$

Here the relations $D = \varepsilon E$, $B = \mu H$ and $k_o = \omega/c = 2\pi/\lambda_o$, where λ_o is the free space wavelength, have been used.

A homogeneous plane wave in a medium of refractive index $\eta = \sqrt{\varepsilon\mu}$ may be represented in a very general manner by

$$E = E_o(r)e^{ik_oP(r,\theta)} \qquad H = H_1(r)e^{ik_oP(r,\theta)}, \tag{15}$$

where $P(r,\theta)$ is the optical path in terms of two spherical coordinates, (r,θ) and E_1 and H_1 are functions of position. Using vector relations for curl and divergence, the

equations (15) become

$$\text{curl } H = \left[\text{curl } H_1 + ik_o(\text{grad } PXH_1)\right] e^{ik_oP} \tag{16}$$

$$\text{div } \mu H = \left[\mu \text{div } H_1 + (H_1 \cdot \text{grad } \mu) + ik_o(\mu H_1 \cdot \text{grad } P)\right] e^{ik_oP}, \tag{17}$$

$$\text{curl } E = \left[\text{curl } E_1 + ik_o(\text{grad } PXE_1)\right] e^{ik_oP}, \tag{18}$$

$$\text{div } \varepsilon E = \left[\varepsilon \text{div } E_1 + (E_1 \cdot \text{grad } \varepsilon) + ik_o\mu(E_1 \cdot \text{grad } P)\right] e^{ik_oP}. \tag{19}$$

Upon substitution of equations (16)-(19) into Maxwell's ecuations (11)-(15),

$$(\text{grad } PXH_1) + \varepsilon E_1 = -\frac{1}{ik_o} \text{curl } H_1, \tag{20}$$

$$(\text{grad } PXE_1) - \mu H_1 = -\frac{1}{ik_o} \text{curl } E_1, \tag{21}$$

$$(E \cdot \text{grad } P) = -\frac{1}{ik_o}\left[(E_1 \cdot \text{grad } \log\varepsilon) + \text{div } E_1\right], \tag{22}$$

$$(H \cdot \text{grad } P) = -\frac{1}{ik_o}\left[(H_1 \cdot \text{grad } \log\mu) + \text{div } H_1\right]. \tag{23}$$

Solution of (20)-(23) as $\lambda \longrightarrow 0$ implies that the right sides of the equations become negligibly small or

$$(\text{grad } PXH_1) + \varepsilon E_1 = 0, \tag{24}$$

$$(\text{grad } PXE_1) - \mu H_1 = 0, \tag{25}$$

$$(E_1 \cdot \text{grad } P) = 0, \tag{26}$$

$$(H_1 \cdot \text{grad } P) = 0. \tag{27}$$

Solving for H_1 from (25) and substituting in (24),

$$\frac{1}{\mu}\left[(E_1 \cdot \text{grad } P)\text{grad } P - E_1(|\text{grad } P|)^2 + \varepsilon E_1\right] = 0. \tag{28}$$

But from (26), (E_1·grad P) is zero and therefore

$$|\text{grad } P|^2 = \eta^2. \qquad (29)$$

The surfaces $P(r,\theta)$ = constant are called the geometrical wave surfaces or the geometrical wavefronts. Geometrical light rays are accordingly defined as the orthogonal trajectories to the wavefronts $P(r,\theta)$ = constant.

The implications of (29) are as follows. Assume that a plane wave has been reflected by the ionosphere and is incident on an irregularity which is characterised by some $P(r,\theta)$. The wavefront will transform from a straight line in such a way that equation (29) is satisfied. In other words, the surface of constant phase will become an irregular curve. Upon emergence from the irregularity, the wavefront will propagate so that the structure at the ground will be some multiple of the structure at the layer. Geometrical optics does not consider interaction of the rays to occur at any place other than the observing plane.

It is possible, therefore, to visualise a mechanism which produces an irregular ground pattern which varies in time by consideration of a moving irregularity and geometrical optics. The shortcomings of this approach are, however, manifest. In the first place, there is no evidence that the irregularity size is so large that wavelength can be neglected at 300 kc/s. Upon this assumption of course, depends the neglect of spreading, or diffraction effects, and scattering as previously defined. These

obvious shortcomings necessitate the rigorous approach which follows.

B. CONCEPT OF AN ANGULAR SPECTRUM AND ITS APPLICATION TO DIFFRACTION PROBLEMS

The Cartesian components of E and H in a wave satisfy the equation

$$\nabla^2 V(r,t) = \frac{1}{c^2} \frac{\partial^2 V}{\partial t^2} (r,t), \tag{30}$$

where $V(r,t)$ refers to each rectangular component of the field vectors. For the two-dimensional case since

$$\frac{\partial^2 V}{\partial t^2} = -\omega^2 V \tag{31}$$

and

$$\frac{-\omega^2}{c^2} = -k^2, \tag{32}$$

the wave equation is simply

$$\frac{\partial^2 V}{\partial x^2} + \frac{\partial^2 V}{\partial y^2} + k^2 V = 0. \tag{33}$$

A fundamental solution of (33) is of the form

$$V = e^{ikr \cos(\theta-\alpha)}, \tag{34}$$

where r, $0 \leq \theta \leq 2\pi$ are polar coordinates related to the Cartesian components by

$$x = r \cos\theta, \tag{35}$$

$$y = r \sin\theta \tag{36}$$

and α is the angle between the direction of propagation and the x axis.

Whittaker and Watson[23] have shown that any solution of (33) can be put in the form of an angular spectrum of plane waves denoted by

$$V = \int F(\alpha) e^{ikr \cos(\theta-\alpha)} d\alpha \qquad (37)$$

by a proper choice of the function $F(\alpha)$ and the path of integration.

As an example of the solution of the wave equation (33) by an angular spectrum, consider a plane wave incident on an infinitely thin conducting sheet situated at $y = 0$. Assume further that a current sheet is induced by the wave which has only one component, J_z, and that this current sheet is responsible for re-radiating waves into the half plane $y > 0$ (see Figure 18). This current sheet can be considered as a diffracting plane interposed between the observer and the wave source.

A solution of Maxwell's curl equations shows that the tangential component of E is continuous in crossing an infinitely thin current sheet while the tangential component of H is discontinuous. In particular, the discontinuity in H is in the tangential component normal to the current density J and is of magnitude

$$J_T = \frac{4\pi}{c} J. \qquad (38)$$

For the case of a current sheet located at $y = 0$ with the single component J_z, there are two components of H, and from symmetry

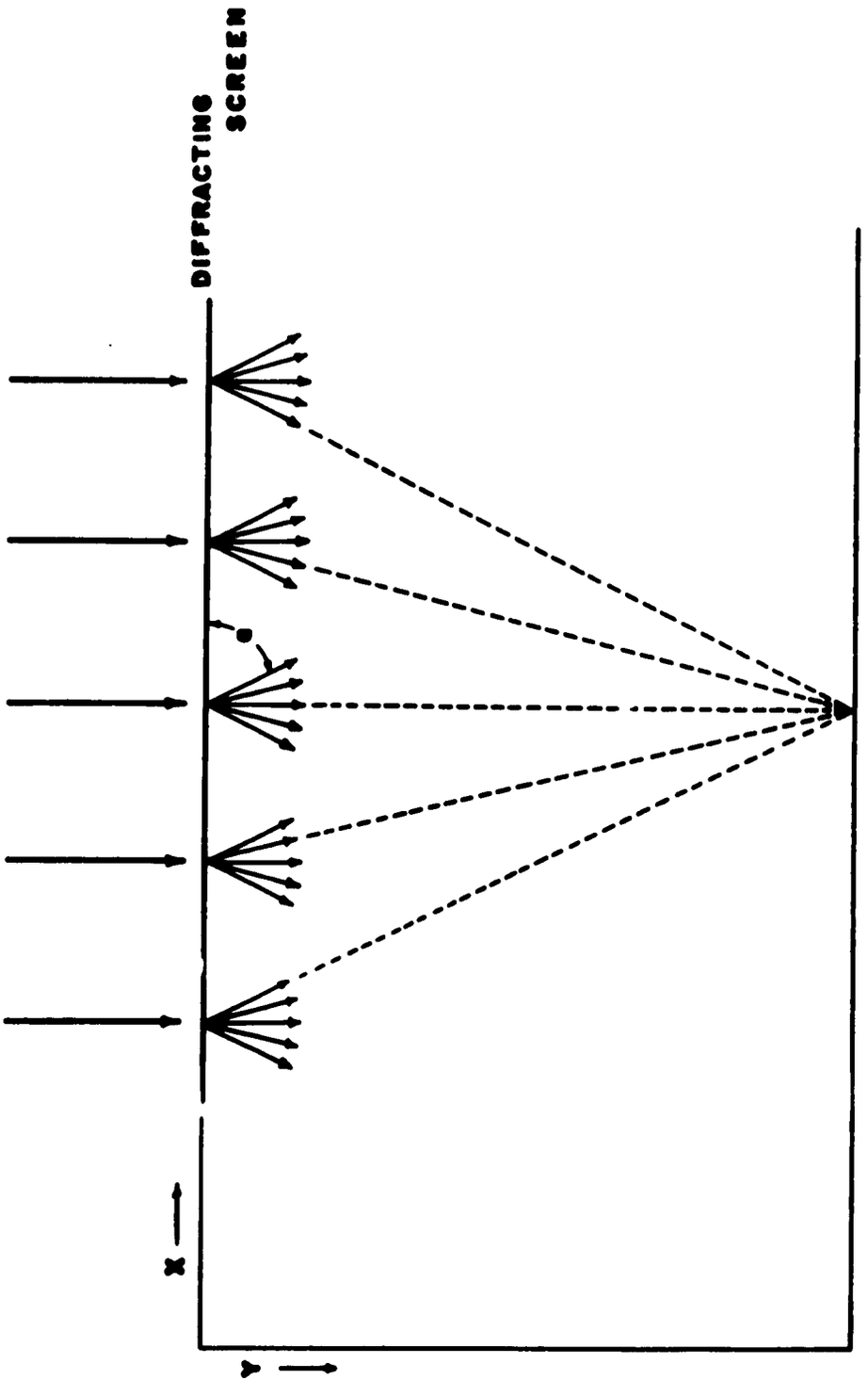

CONCEPT OF AN ANGULAR SPECTRUM

FIGURE 18

$$H_x = \mp \frac{2\pi}{c} J_z \tag{39}$$

with the upper or lower sign depending on whether y reaches zero through positive or negative values respectively.

The problem of ionospheric diffraction can now be formulated with a current sheet model. If a ground transmitted wave is reflected by the ionosphere and is incident on an irregularity which is considered as a conducting sheet, currents are induced which give rise to re-radiated waves.

In particular, assume that the wave denoted by

$$E = (0,0,1)e^{ikr\ \cos(\theta-\alpha)} \tag{40}$$

and

$$H = (\sin\alpha,-\cos\alpha,0)e^{ikr\ \cos(\theta-\alpha)} \tag{41}$$

is radiated into the half space $y > 0$ by an induced current J_z. It can be readily seen that a current given by

$$J_z = \frac{-c}{2\pi} e^{ikr\ \cos(\theta-\alpha)} \sin\alpha \tag{42}$$

satisfies equation (39) for H_x given by (41). In particular, at $y = 0$

$$J_z(x,0) = \frac{-c}{2\pi} e^{ikx\ \cos\alpha} \sin\alpha. \tag{43}$$

Since any current distribution can be built up by an appropriate superposition of (43), assume that the current distribution is given by

$$J_z(x,0) = \frac{-c}{2\pi}\int_{-\infty}^{\infty} P(\beta)e^{ikx\beta}d\beta. \tag{44}$$

The change of variable

$$\beta = \cos\alpha \tag{45}$$

in (44) gives

$$J_z(x,0) = \frac{-c}{2\pi}\int_c \sin\alpha P(\cos\alpha) e^{ikx\cos\alpha} d\alpha, \tag{46}$$

where c denotes the path along which $\cos\alpha$ ranges through real values from $-\infty$ to ∞. At some distance y from the screen the phase factor will have an additional contribution from $y\sin\alpha$ or

$$J_z(x,y) = \frac{-c}{2\pi}\int_c \sin\alpha P(\cos\alpha) e^{ikr\cos(\theta-\alpha)} d\alpha. \tag{47}$$

From (39) it is evident that

$$H_x(x,y) = \pm \int_c \sin\alpha P(\cos\alpha) e^{ikr\cos(\theta\mp\alpha)} d\alpha \tag{48}$$

with the upper sign for $y>0$ and the lower sign for $y<0$.

For the two-dimensional wave equation solution such as is being considered here, it is also true that

$$H_x = \frac{1}{ik}\frac{\partial E_z}{\partial y} \tag{49}$$

and

$$H_y = \frac{1}{ik}\frac{\partial E_z}{\partial x}. \tag{50}$$

For the particular wave polarization being considered, the remaining two non-zero field components are therefore

$$H_y(x,y) = -\int_c \cos\alpha P(\cos\alpha) e^{ikr\cos(\theta\mp\alpha)} d\alpha \tag{51}$$

and

$$E_z(x,y) = \int_c P(\cos\alpha) e^{ikr\ \cos(\theta \mp \alpha)} d\alpha. \tag{52}$$

It is of interest to consider the value of $E_z(x,0)$. This is given by

$$E_z(x,0) = \int_{-\infty}^{\infty} P(\cos\alpha) e^{ikx\ \cos\alpha} d\alpha. \tag{53}$$

By the theory of Fourier transforms,

$$P(\cos\alpha) = \int_{-\infty}^{\infty} E_z(x,0) e^{-ikx\ \cos\alpha} dx. \tag{54}$$

Equations (53) and (54) may be summarized by stating that when a one-dimensional diffracting screen is illuminated by a monochromatic wave, the angular spectrum produced, expressed in terms of the cosine of the angle between the wavefront and the x axis, is the Fourier transform of the distribution of complex amplitude over the wavefront just as it leaves the screen (see Figure 18).

Using the substitutions

$$c = \cos\alpha \tag{55}$$

and

$$s = \sin\alpha, \tag{56}$$

equation (52) can be rewritten

$$E_z(x,y) = \int_c P(c) e^{ik(xc+ys)} d\alpha. \tag{57}$$

The plane waves corresponding to the limits of integration along the real axis are homogeneous and radiate into the regions $y>0$, $y<0$. The imaginary limits give

rise to inhomogeneous waves.

For example, if

$$\alpha = \alpha_1 + i\alpha_2, \tag{58}$$

then

$$e^{ikr\cos(\theta-\alpha)} = e^{ikr\cosh\alpha_2\cos(\theta-\alpha_1)}e^{-kr\sinh\alpha_2\sin(\theta-\alpha_1)}, \tag{59}$$

indicating that the equiamplitude and equiphase planes are mutually perpendicular. In this case the directions of phase propagation are along the positive and negative x directions, and the amplitudes are attenuated exponentially in the direction normal to and away from y = 0. These waves are called evanescent waves and on the average carry no energy away from the screen.

From comparison of equations (53) and (52), it is apparent that E_z, in traveling the distance from (0,0) to $(0,y_o)$, undergoes a phase retardation of amount $\Delta\phi$ where

$$\Delta\phi = ksy_o. \tag{60}$$

Since

$$s = (1-c^2)^{\frac{1}{2}}, \tag{61}$$

$$\Delta\phi \simeq ky_o - \frac{k}{2}y_oc^2. \tag{62}$$

The component ky_o represents the phase delay of the undiffracted wave in traveling the distance y_o and $-\frac{k}{2}y_oc^2$ represents an additional phase gain which is undergone by the component of the angular spectrum traveling in the direction c. For $\alpha < 10^o$ equation (62) is fairly exact.

In other words, if g(x) represents the distribution of complex amplitude in the diffraction pattern at y_o with the phase referred to $(0,y_o)$, then g(x) is formed by the same angular spectrum at the diffracting screen, but the phase of each component is advanced by an amount $\frac{k}{2} y_o c^2$ for $\alpha < 10^o$. Employing the notation used by Ratcliffe[15] to symbolise Fourier transforms, this relationship may be denoted by

$$g(x) \leftrightarrow F(c)e^{-i \frac{k}{2} y_o c^2} = G(c), \tag{63}$$

where G(c) represents the angular spectrum referred to the point $(0,y_o)$.

C. THE GENERALIZED SPATIAL AUTOCORRELATION FUNCTION AND THE WIENER-KHINTCHINE THEOREM

If a complex amplitude function F(x) has a mean value of zero, it is sometimes convenient to use its generalized spatial autocorrelation function defined by

$$\rho(\gamma) = \frac{\int_{-\infty}^{\infty} F(x)F^*(x+\gamma)dx}{\int_{-\infty}^{\infty} F(x)F^*(x)dx}, \tag{64}$$

where the asterisk indicates the complex conjugate. In particular, if F(x) is equal to $E_z(x,0)$, then

$$\rho(\gamma) = \frac{\int_{-\infty}^{\infty} |P(c)|^2 e^{ikc} dc}{\int_{-\infty}^{\infty} |P(c)|^2 dc}. \tag{65}$$

If F(x) and g(x) are the complex amplitude

distributions over the screen and the observing plane respectively, then using the previously defined notation for Fourier transforms, the following relations are evident:

$$F(x) \leftrightarrow P(c), \tag{66}$$

$$\rho_f(\tau) \leftrightarrow |P(c)|^2, \tag{67}$$

$$g(x) \leftrightarrow P(c)e^{-i\frac{k}{2}y_0c^2}, \tag{68}$$

and

$$\rho_g(\tau) \leftrightarrow \left|P(c)e^{-i\frac{k}{2}y_0c^2}\right|^2, \tag{69}$$

or

$$\rho_g(\tau) \leftrightarrow |P(c)|^2. \tag{70}$$

Equations (67) and (70) show that the generalized spatial autocorrelation function is invariant with the distance of the observer from the screen.

D. EXTENSION TO A TWO-DIMENSIONAL SCREEN

The foregoing analysis may be extended to the diffraction effects produced when monochromatic radiation is incident on a two-dimensional conducting plane. If one assumes, for example, that the induced current J has two components, a two-dimensional Fourier integral can be used to represent it and subsequently yield the two-dimensional representation of field components. In addition, the wave equation must be solved in three dimensions.

However, since this study is primarily an investigation into methods of recording and analyzing diffraction patterns rather than a detailed investigation into

their causes, the two-dimensional diffraction pattern will not be discussed.

CHAPTER V

SUMMARY AND CONCLUSIONS

The specific problem to be solved in this study is the development of a technique for studying the angular spectrum of ionospherically reflected waves. The large body of investigations dealt with in Chapter II indicates that fluctuations in the amplitude and phase of ionospherically reflected waves are caused by irregularities or dense patches of ionization in motion in the ionosphere. A form of representation of these irregularities is a thin diffracting screen. Waves incident on such a screen are reradiated in the form of an angular spectrum of plane waves which can be reconstructed at the ground to yield information about the irregularity.

The wide aperture, high directivity, scanned antenna array developed in the course of this study provides a ready means of detecting the angular spectrum. The basic unit of the array is a semiconductor switch which permits rapid sequential sampling of six antennas in a linear array. By means of a phase locked oscillator arrangement, the phase as well as the amplitude of the signal received at each antenna can be continuously recorded.

Records have been taken with the switched antenna array, and a comparison with independent work in the field indicates that the preliminary results are compatible with other findings.

A. SUGGESTIONS FOR FURTHER WORK

First a larger number of records must be obtained to compare with independent findings. The short samples discussed in this study are insufficient to generalize comprehensive results. The method of reduction of these records should be changed, moreover, from the laborious visual method to a digital paper punch arrangement which can be sampled rapidly by a high speed computer.

In addition, the problem of anomalous propagation of the ground wave in phase measurements should be removed. A method of accomplishing this could be instrumented as follows. A 300 kc/s receiving antenna located at the instrumentation building would phase lock an oscillator at 300 kc/s in the same manner as the 1400 kc/s oscillator is presently locked. By means of delay circuitry a portion of this oscillator would be gated for 200 μsec after the trailing edge of the ground pulse. This gated pulse would then be radiated along the antenna line and would serve, in turn, to phase lock the existing oscillator for phase measurements of the sky wave. An additional gate would be provided to prevent the Scotia ground pulse from phase locking the sky wave oscillator reference. This method would permit an exact determination of the angle of arrival of the phase lock signal at each antenna.

BIBLIOGRAPHY

[1]Ratcliffe, J. A. and Pawsey, J. L., Proc. Camb. Phil. Soc. 29, 301 (1933).

[2]Pawsey, J. L., Proc. Camb. Phil. Soc. 31, 125 (1935).

[3]Ratcliffe, J. A., Nature 152, 9 (1948).

[4]Rice, S. O., Bell Syst. Tech Jour. 23, 282 (1944).

[5]Booker, H. G., Ratcliffe, J. A. and Shinn, D. H., Phil. Trans. A242, 579 (1950).

[6]Booker, H. G. and Clemmow, P. C., Proc. Instn. Elec. Engrs. 97, 18 (1950).

[7]Briggs, B. H., Phillips, G. J. and Shinn, D. H., Proc. Phys. Soc. B63, 106 (1950).

[8]Bramley, E. N., Proc. Instn. Elec. Engrs. III 98, 98 (1951).

[9]Hewish, A., Proc. Roy. Soc. A209, 81 (1951).

[10]Hewish, A., Proc. Roy. Soc. A214, 494 (1952).

[11]Fejer, J. A., Proc. Roy. Soc. A220, 455 (1953).

[12]Bramley, E. N., Proc. Roy. Soc. A225, 515 (1954).

[13]Jones, R. E., Millman, G. H. and Nertney, R. J., Jour. Atmos. Terr. Phys. 3, 79 (1953).

[14]Bowhill, S. A., Scientific Report No. 89, Ionosphere Research Laboratory, The Pennsylvania State University (1956).

[15]Ratcliffe, J. A., Rep. Prog. Phys. 19, 188 (1956).

[16]Houston, E. H., Scientific Report No. 93, Ionosphere Research Laboratory, The Pennsylvania State University (1957).

[17]Pitteway, M. L. V., Proc. Roy. Soc. A246, 556 (1958).

[18]Bowhill, S. A., Jour. Atmos. Terr. Phys. 20, 9 (1961).

[19]Bowhill, S. A., Jour. Res. Natl. Bur. Stds. 65D, 275 (1960).

[20]Hargreaves, J. K., Jour. Atmos. Terr. Phys. 20, 155 (1960).

[21]Jordan, E. C., Electromagnetic Waves and Radiating Systems, Prentice Hall, Inc. (1961), p. 572.

[22]Lee, H. S., Private Communication.

[23]Whittaker, E. T. and Watson, G. N., Modern Analysis, Cambridge University Press (1928), p. 397.